

M.MS.IPL

by 93

MSFC

MTP-P&VE-F-63-8

May 2, 1963

GPO PRICE \$ _____

CFSTI PRICE(S) \$ _____

Hard copy (HC) 2.00

Microfiche (MF) 5.0

ff 653 July 65

GEORGE C. MARSHALL FLIGHT CENTER

HUNTSVILLE, ALABAMA

PARAMETRIC PERFORMANCE ANALYSIS OF LUNAR MISSIONS

Part II: Lunar Descent

By Charles M. Akridge and Sam H. Harlin

FACILITY FORM 602

N66-12869

(ACCESSION NUMBER)

39

(PAGES)

TMX-56960

(NASA CR OR TMX OR AD NUMBER)

(THRU)

8

(CODE)

30

(CATEGORY)



FOR INTERNAL USE ONLY

NATIONAL AERONAUTICS AND SPACE ADMINISTRATION

GEORGE C. MARSHALL SPACE FLIGHT CENTER

MTP-P&VE-F-63-8

PARAMETRIC PERFORMANCE ANALYSIS OF LUNAR MISSIONS

PART II

LUNAR DESCENT

By

Charles M. Akridge and Sam H. Harlin

ABSTRACT

12869

The effect of thrust-to-weight ratios, and apocenter altitude on trajectory parameters has been investigated for descent to the lunar surface from parking orbit. A single stage with constant thrust directed against the velocity vector was used in all instances. Specific impulses of 300 and 420 sec were used for comparison.

The purpose of this report is to present trajectory parameters for the powered lunar landing maneuver from various lunar orbit altitudes. The results of the study show the variation of trajectory parameters for earth thrust-to-weight ratios from 0.2 to 0.5. These parameters include: true anomaly at initiation of powered descent; change in altitude, flight path angle and range angle during thrusting; burning time, characteristic velocity and velocity losses.

Author

GEORGE C. MARSHALL SPACE FLIGHT CENTER

MTP-P&VE-F-63-8

PARAMETRIC PERFORMANCE ANALYSIS OF LUNAR MISSIONS

PART II

LUNAR DESCENT

By

Charles M. Akridge and Sam H. Harlin

FLIGHT OPERATIONS SECTION
ADVANCED FLIGHT SYSTEMS BRANCH
PROPULSION AND VEHICLE ENGINEERING DIVISION

TABLE OF CONTENTS

	Page
SUMMARY	1
SECTION I. INTRODUCTION.	1
SECTION II. ANALYSIS	2
SECTION III. ASSUMPTIONS.	6
SECTION IV. RESULTS AND CONCLUSIONS	6
SECTION V. GRAPHIC PRESENTATION	9
BIBLIOGRAPHY.	34

LIST OF ILLUSTRATIONS

Figure	Title	Page
1	Apocenter and Pericenter Velocities Versus Apocenter and Pericenter Altitudes	10
2	Chart for Determining Elevation and Slant Range of Lunar Spacecraft (0 to 1100 km)	11
3	Characteristic Velocity as a Function of Propellant Mass Fraction and Specific Impulse.	12
4	Characteristic Impulse Velocity to Attain Transfer Ellipse with $r_p = 1748.3$ km	13
5	Characteristic Velocity for Lunar Descent	
	a. $I_{sp} = 300$ sec	14
	b. $I_{sp} = 420$ sec	15
6	Propellant Mass Fraction for Lunar Descent	
	a. $I_{sp} = 300$ sec	16
	b. $I_{sp} = 420$ sec	17
7	Change in Altitude for Lunar Descent	
	a. $I_{sp} = 300$ sec	18
	b. $I_{sp} = 420$ sec	19
8	Change in Flight Path Angle for Lunar Descent	
	a. $I_{sp} = 300$ sec	20
	b. $I_{sp} = 420$ sec	21

LIST OF ILLUSTRATIONS (Concluded)

Figure	Title	Page
9	Change in Central Angle for Lunar Descent	
	a. $I_{sp} = 300 \text{ sec}$	22
	b. $I_{sp} = 420 \text{ sec}$	23
10	Surface Range for Lunar Descent	
	a. $I_{sp} = 300 \text{ sec}$	24
	b. $I_{sp} = 420 \text{ sec}$	25
11	True Anomaly at Initiation of Lunar Descent	
	a. $I_{sp} = 300 \text{ sec}$	26
	b. $I_{sp} = 420 \text{ sec}$	27
12	Burning Time for Lunar Descent	
	a. $h_a = 50 \text{ km}$	28
	b. $h_a = 100 \text{ km}$	29
	c. $h_a = 200 \text{ km}$	30
	d. $h_a = 300 \text{ km}$	31
13	Velocity Losses for Lunar Descent	
	a. $I_{sp} = 300 \text{ sec}$	32
	b. $I_{sp} = 420 \text{ sec}$	33

DEFINITION OF SYMBOLS

Symbol	Definition
F	Thrust, kp
g	Gravitational acceleration, m/sec ²
g _e	Earth gravitational acceleration, 9.80665 m/sec ²
h	Altitude, km
Δh	Altitude change, h - h ₀ , km
I _{sp}	Specific impulse, sec
m	Mass, $\frac{kp - sec^2}{m}$
r	Radius, km
t	Time, sec
Δt	Incremental time, sec
S	Surface range, km
V	Velocity, m/sec
V*	Comparative velocity, m/sec
ΔV	Stage characteristic velocity increment, m/sec
W ₀	Gross weight, kp
F/W ₀	Initial thrust-to-weight ratio (based on weight at sea level)
W ₈	Propellant weight, kp
x	Range, km
α	Thrust vector orientation angle measured from the velocity to the thrust vector (positive down), deg
ξ	Propellant mass fraction, W ₈ / W ₀
β	Flight path angle from vertical, deg
Δβ	Change in flight path angle, deg
μ _e	Gravitational constant for the moon, 4906 km ³ /sec ²

DEFINITION OF SYMBOLS (Concluded)

Symbol	Definition
ν	True anomaly, deg
ψ	Central angle from arbitrary reference, deg
$\Delta\psi$	Central angle change, $\psi - \psi_0$, deg
Subscripts	
a	Apocenter
B	Burnout
e	Earth
ex	Exhaust
f	Final
id	Ideal
o	Initial
p	Pericenter
c	Moon

GEORGE C. MARSHALL SPACE FLIGHT CENTER

MTP-P&VE-F-63-8

PARAMETRIC PERFORMANCE ANALYSIS OF LUNAR MISSIONS

PART II

LUNAR DESCENT

By

Charles M. Akridge and Sam H. Harlin

SUMMARY

The effect of thrust-to-weight ratios and apocenter altitude on trajectory parameters has been investigated for descent to the lunar surface from parking orbit. A single stage with constant thrust directed against the velocity vector was used in all instances. Specific impulses of 300 and 420 sec were used for comparison.

The results of the study show the variation of trajectory parameters for earth thrust-to-weight ratios from 0.2 to 0.5. These parameters include: true anomaly at initiation of powered descent; change in altitude, flight path angle, and range angle during thrusting; burning time, characteristic velocity, and velocity losses.

SECTION I. INTRODUCTION

Orbital operations are of great interest in lunar exploration because of requirements imposed by the landing site, energy and tracking. Preliminary analysis of lunar missions requires a rapid method of sufficient accuracy for determining trajectory parameters.

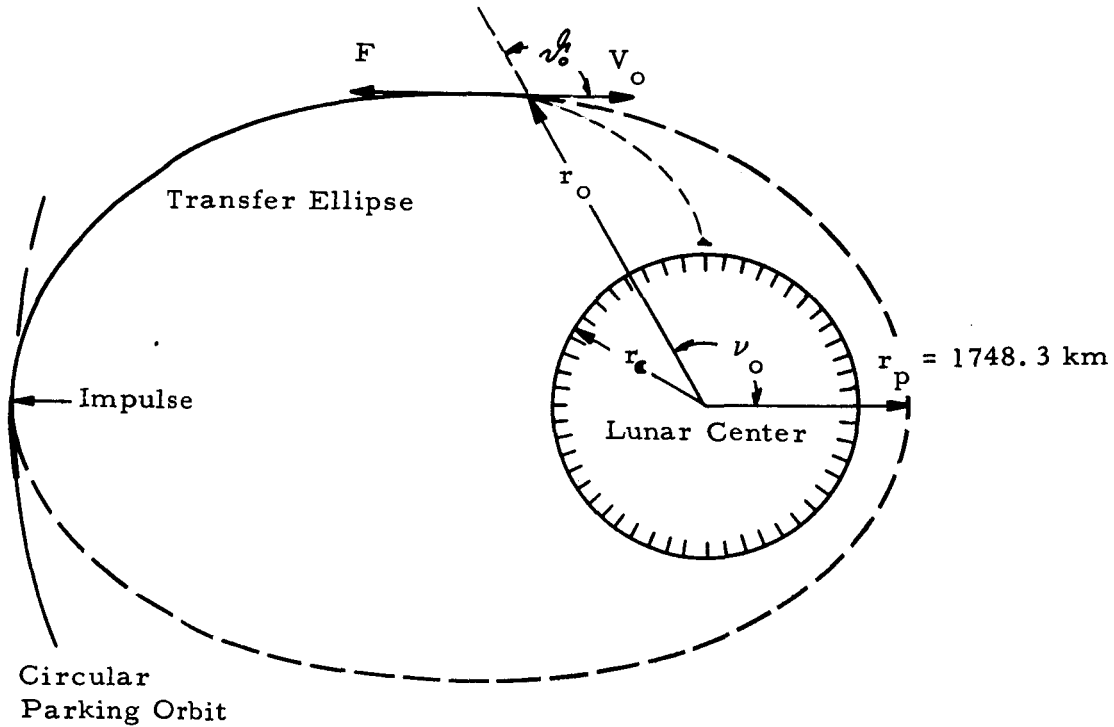
The purpose of this report is to present trajectory parameters for the powered lunar landing maneuver from various lunar orbit altitudes. The parameters presented are: velocity, altitude change,

surface range, change in flight path angle, change in central angle, true anomaly, burning time, propellant mass fraction and velocity losses.

The approach used was to apply an impulse in the parking orbit to attain a transfer ellipse with a 10-kilometer pericenter altitude. At the proper point on the transfer ellipse, powered braking was initiated to arrive at a 300-meter altitude with the zero velocity. The equations of motion were integrated on a RECOMP II computer, using Runge-Kutta numerical integration.

SECTION II. ANALYSIS

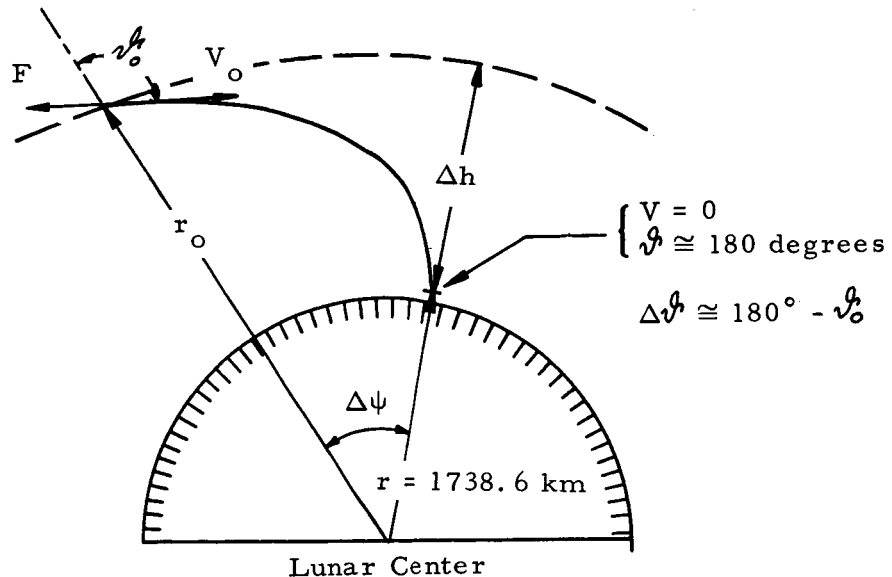
One method of landing on the lunar surface is to direct the thrust against the velocity vector ($\alpha = 180^\circ$) and follow a gravity turn path. The sketch below illustrates the conditions at initiation of burning.



First, an impulse (as calculated from FIG 1) was applied against the velocity vector to attain the transfer ellipse. The pericenter altitude of the transfer ellipse was taken as 10 km to insure against collision

with the surface if powered descent was not initiated. This pericenter altitude was selected because of surface irregularities, guidance errors, retro-thrust errors, etc. From a performance view, it is preferable to expend the energy at as low an altitude as possible.

The initial true anomaly (measured from the undisturbed Keplerian pericenter radius) varies with thrust-to-weight ratio and parking orbit altitude. It is seen that as parking orbit altitude decreases the initial true anomaly will increase (to a maximum of 180°).



The sketch above shows the initial and final trajectory parameters, as well as change in flight path angle, altitude, and central range angle. The line of sight and angular range can be determined from FIG 2, using initial conditions. The equations of motion were numerically integrated from initial conditions to 300-meters above the surface. The initial conditions were found by iteration to give the desired end conditions.

The following point mass, planar equations of motion were used with $\alpha = 180^\circ$ in all instances.

$$\dot{V} = \frac{F \cos \alpha}{m} - \frac{g_e r_e^2}{r^2} \cos \vartheta \quad (1)$$

$$\dot{V} = \frac{F \sin \alpha}{m} + \left[\frac{g_e r_e^2}{r^2} - \frac{v^2}{r} \right] \sin \vartheta \quad (2)$$

$$\dot{r} = V \cos \vartheta \quad (3)$$

$$\dot{\psi} = \frac{V \sin \vartheta}{r} \quad (4)$$

where

$$m = m_0 + \int \dot{m} dt \quad (5)$$

and

$$\dot{m} = - \frac{F}{V_{ex}} \quad (6)$$

The velocity and flight path angle may be obtained by integrating the equation of motion

$$V = \int \dot{V} dt \quad (7)$$

$$\vartheta = \int \dot{\vartheta} dt \quad (8)$$

The range and pericenter altitude can then be calculated by the relations

$$x = \int \frac{r_e}{r} v \sin \vartheta dt \quad (9)$$

$$h = h_0 + \int \dot{r} dt \quad (10)$$

and the central angle

$$\psi = \int \frac{\dot{x}}{r_e} dt \quad (11)$$

and surface range

$$S = r_e \Delta\psi \quad (12)$$

The initial weight of the vehicle is

$$W_o = W_c + W_s \quad (13)$$

The undisturbed Keplerian true anomaly at initiation of powered descent is

$$\nu_o = \cos^{-1} \left[\frac{(V_a r_a)^2 / \mu_e - r_o}{r_o \sqrt{1 - \frac{V_o^2 r_o}{\mu_e} \left(2 - \frac{V_o^2 r_o}{\mu_e} \right) \sin^2 \nu_o}} \right] \quad (14)$$

The velocity expended by the vehicle is the characteristic velocity, or

$$\Delta V = V_{ex} \ln \left(\frac{1}{1 - \zeta} \right) \quad (15)$$

and may be determined from FIG 3. Consequently, the velocity losses are the difference between the characteristic velocity and the change in comparative velocity, or

$$\Delta V_{loss} = \Delta V - \Delta V^* \quad (16)$$

where the comparative velocity is

$$V^* = \sqrt{V_o^2 + 2\mu_e \left(\frac{1}{r} - \frac{1}{r_o} \right)} \quad (17)$$

and the change in comparative velocity during descent from $r = r_o$ to $r = r_f$ is

$$\Delta V^* = \sqrt{V_o^2 + 2\mu_e \left(\frac{1}{r_f} - \frac{1}{r_o} \right)} - V_f \quad (18)$$

By substituting in original equation for velocity losses

$$\Delta V_{loss} = V_{ex} \ln \left(\frac{1}{1 - \zeta} \right) - \left[\sqrt{V_o^2 + 2\mu_e \left(\frac{1}{r_f} - \frac{1}{r_o} \right)} - V_f \right] \quad (19)$$

SECTION III. ASSUMPTIONS

A summary of the basic assumptions used in this analysis follows:

1. Deceleration of a single stage from a transfer ellipse to a 300 meter (hover) altitude and zero velocity using constant thrust directed against the velocity vector.

2. Initial parking orbit altitudes

$$h = 50 \text{ km}$$

$$h = 100 \text{ km}$$

$$h = 200 \text{ km}$$

$$h = 300 \text{ km}$$

3. For comparison, specific impulses of 300 sec and 420 sec were used.

4. The initial earth thrust-to-weight ratio for a chemical stage was varied parametrically from 0.2 to 0.5.

5. Mean spherical moon

$$\mu_e = 4906 \text{ km}^3/\text{sec}^2$$

$$r_e = 1738.3 \text{ km}$$

SECTION IV. RESULTS AND CONCLUSIONS

The results are shown in FIG 4 through 13. For convenience, most variables are shown as a function of initial vehicle thrust-to-weight ratio.

The characteristic impulse velocity, shown in FIG 4, is the velocity necessary to attain a transfer ellipse from a circular parking orbit altitude. The apocenter altitude of the transfer ellipse is assumed to be circular parking orbit altitude and the pericenter altitude is 10 km in all instances. Since losses were negligible, an impulsive velocity was assumed.

The characteristic velocity for descent to 300-meters above the lunar surface is shown in FIG 5a and 5b for specific impulses of 300 sec and 420 sec, respectively. The corresponding propellant mass fraction is shown in FIG 6a and 6b.

FIG 7a and 7b show the altitude change, Δh , during powered descent for specific impulses of 300 sec and 420 sec, respectively. A limit is reached, for a gravity turn ($\alpha = 180^\circ$), when the altitude change becomes equal to the apocenter altitude. This limit determines the minimum initial thrust-to-weight ratio for continuous burn from parking orbit to 300 m above the surface. This limit is reflected in the change in flight path angle, $\Delta\psi$, FIG 8a and 8b when $\Delta\psi = 90^\circ$.

The change in central angle, $\Delta\psi$ (angular range), during powered descent is given in FIG 9a and 9b. The product of $\Delta\psi$ (in radians) and the mean lunar radius is the surface range and is shown in FIG 10a and 10b. The limit shown for $\Delta\psi$ and S is reached when powered descent is initiated at apocenter.

The true anomaly, ν_0 , shown in FIG 11a and 11b, is measured from the undisturbed Keplerian pericenter radius to the radius at initiation of powered descent. True anomaly equals 180° for the limit of minimum thrust-to-weight ratio. Burning times for the powered descent are given in FIG 12a, 12b, 12c, and 12d. The true gravity losses are shown in FIG 13a and 13b. Burning times and gravity losses are a maximum in the limiting case.

SECTION V. GRAPHIC PRESENTATION

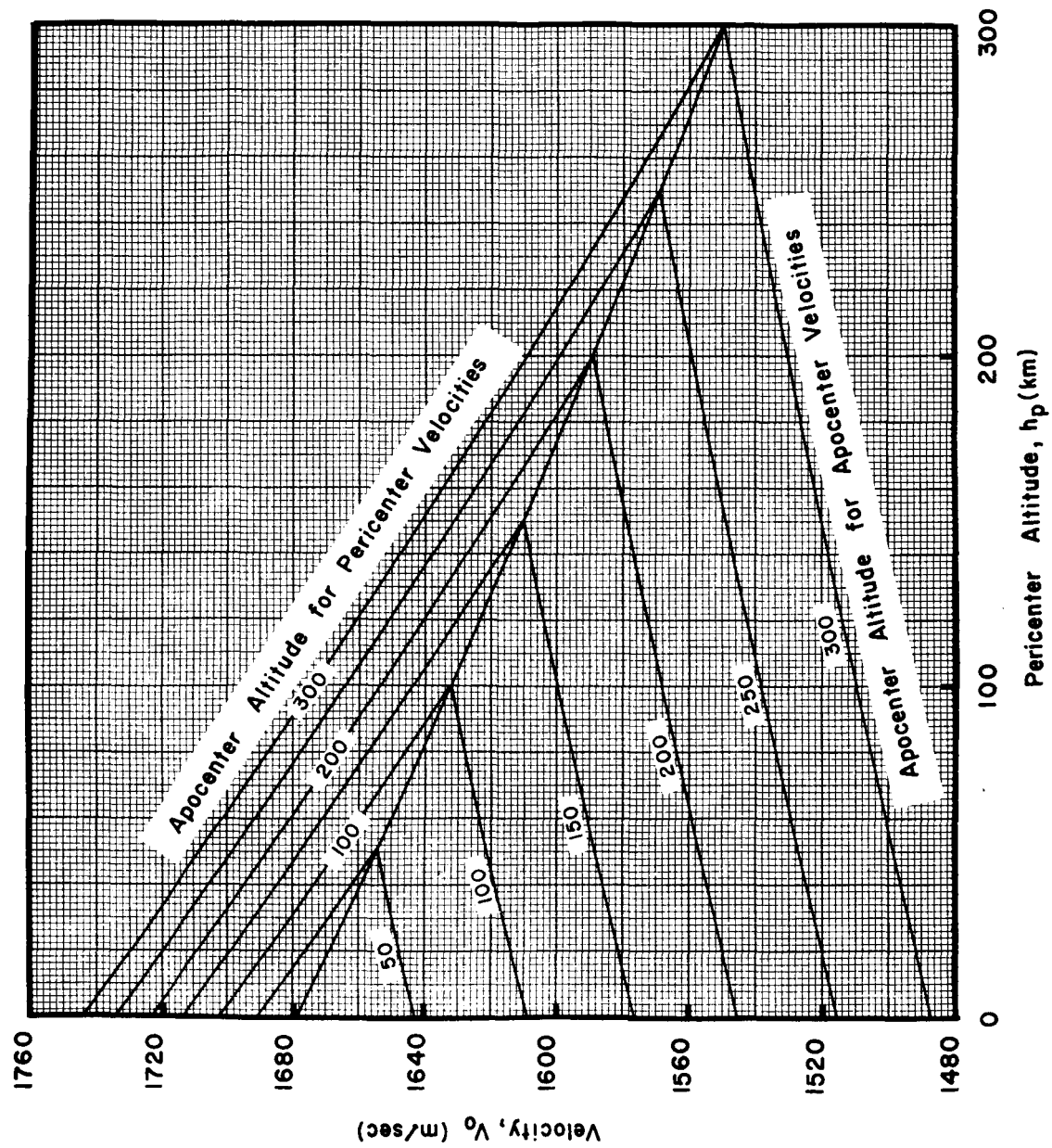


FIGURE 1. APOCENTER AND PERICENTER VELOCITIES VERSUS
APOCENTER AND PERICENTER ALTITUDES

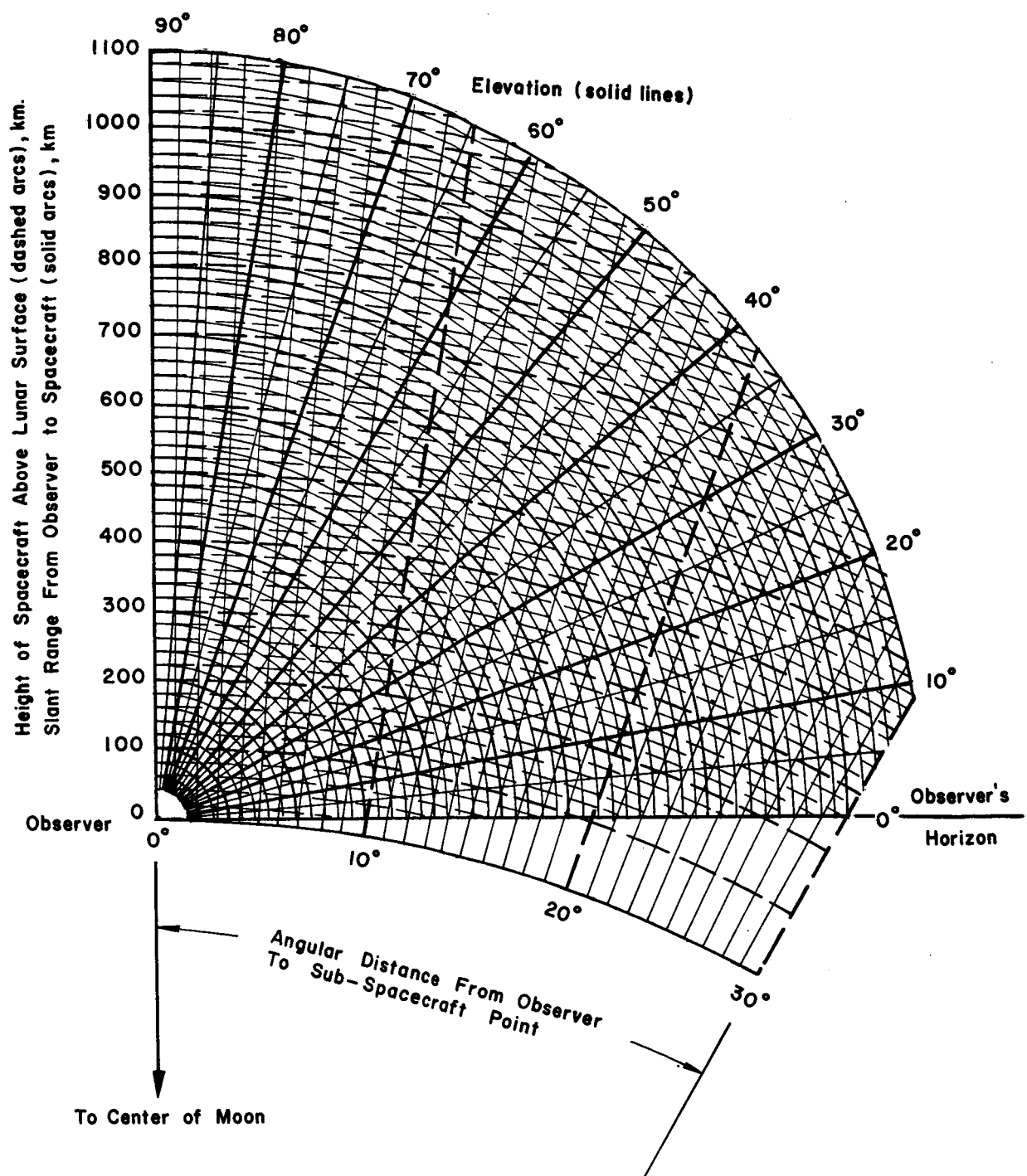


FIGURE 2. CHART FOR DETERMINING ELEVATION AND SLANT RANGE OF LUNAR SPACECRAFT (0 to 1100 km)

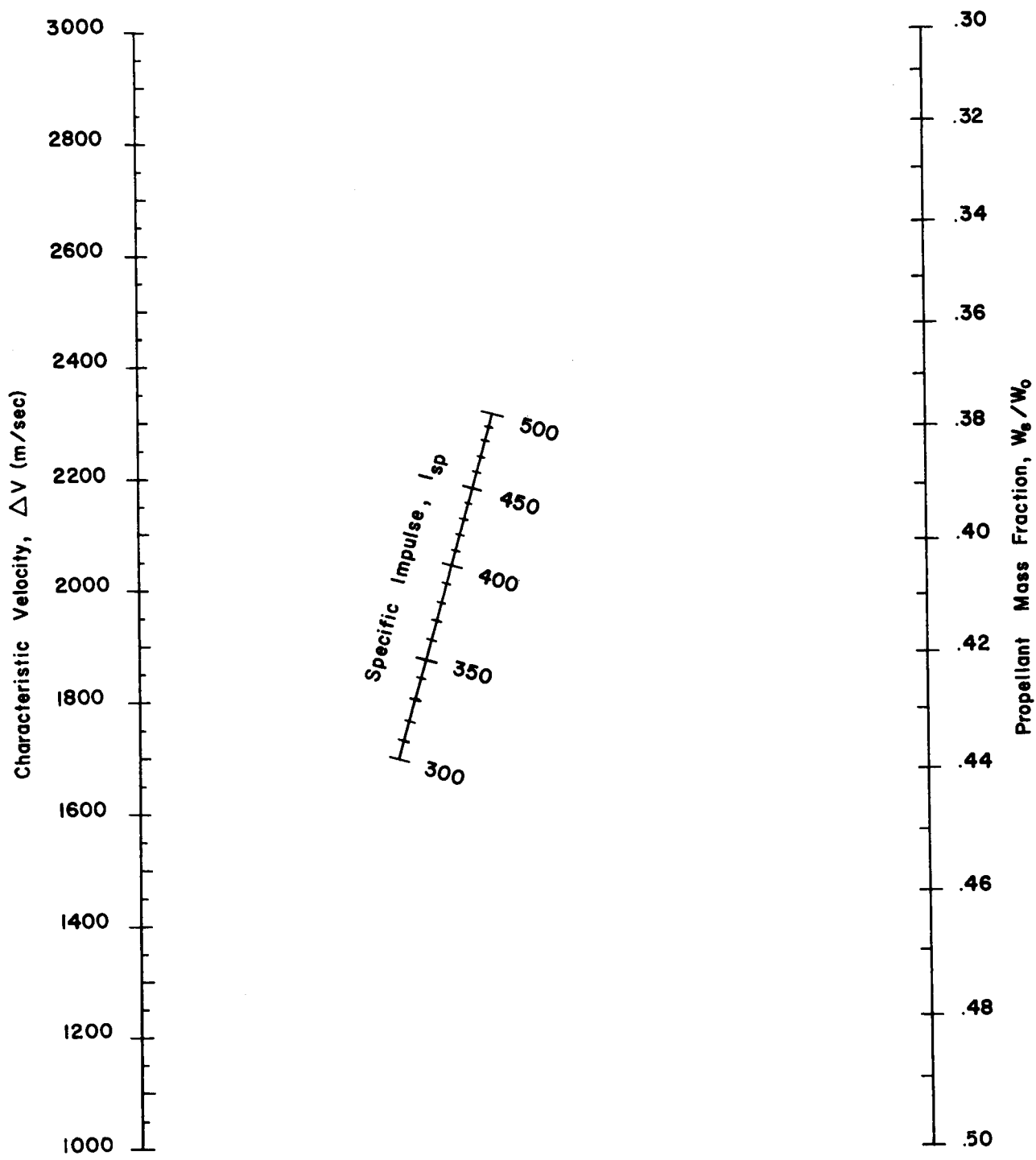


FIGURE 3. CHARACTERISTIC VELOCITY AS A FUNCTION OF PROPELLANT MASS FRACTION AND SPECIFIC IMPULSE

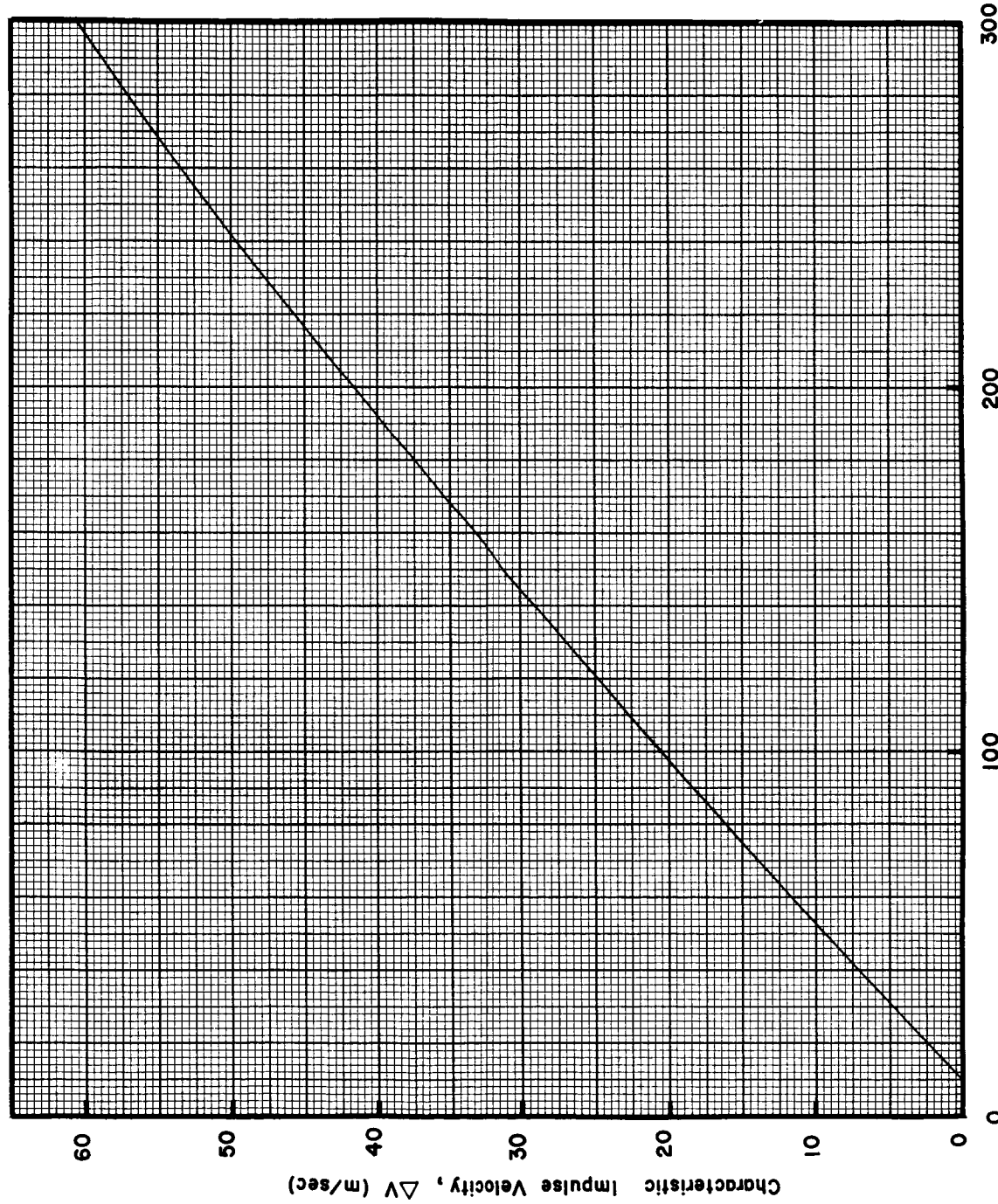


FIGURE 4. CHARACTERISTIC IMPULSE VELOCITY TO ATTAIN TRANSFER ELLIPSE WITH $r_p = 1748.3$ km

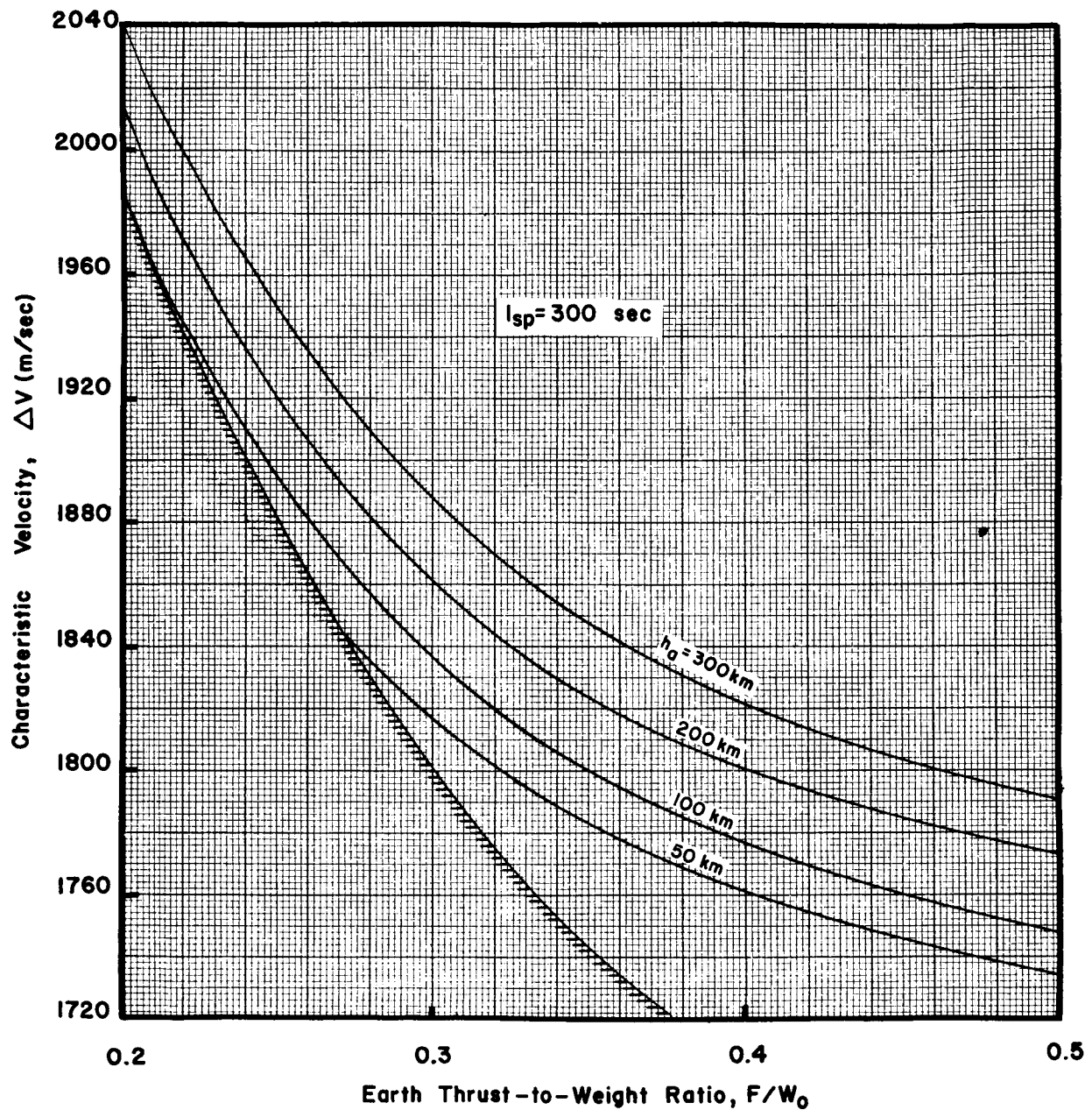


FIGURE 5a. CHARACTERISTIC VELOCITY FOR LUNAR DESCENT - $I_{sp} = 300 \text{ sec.}$

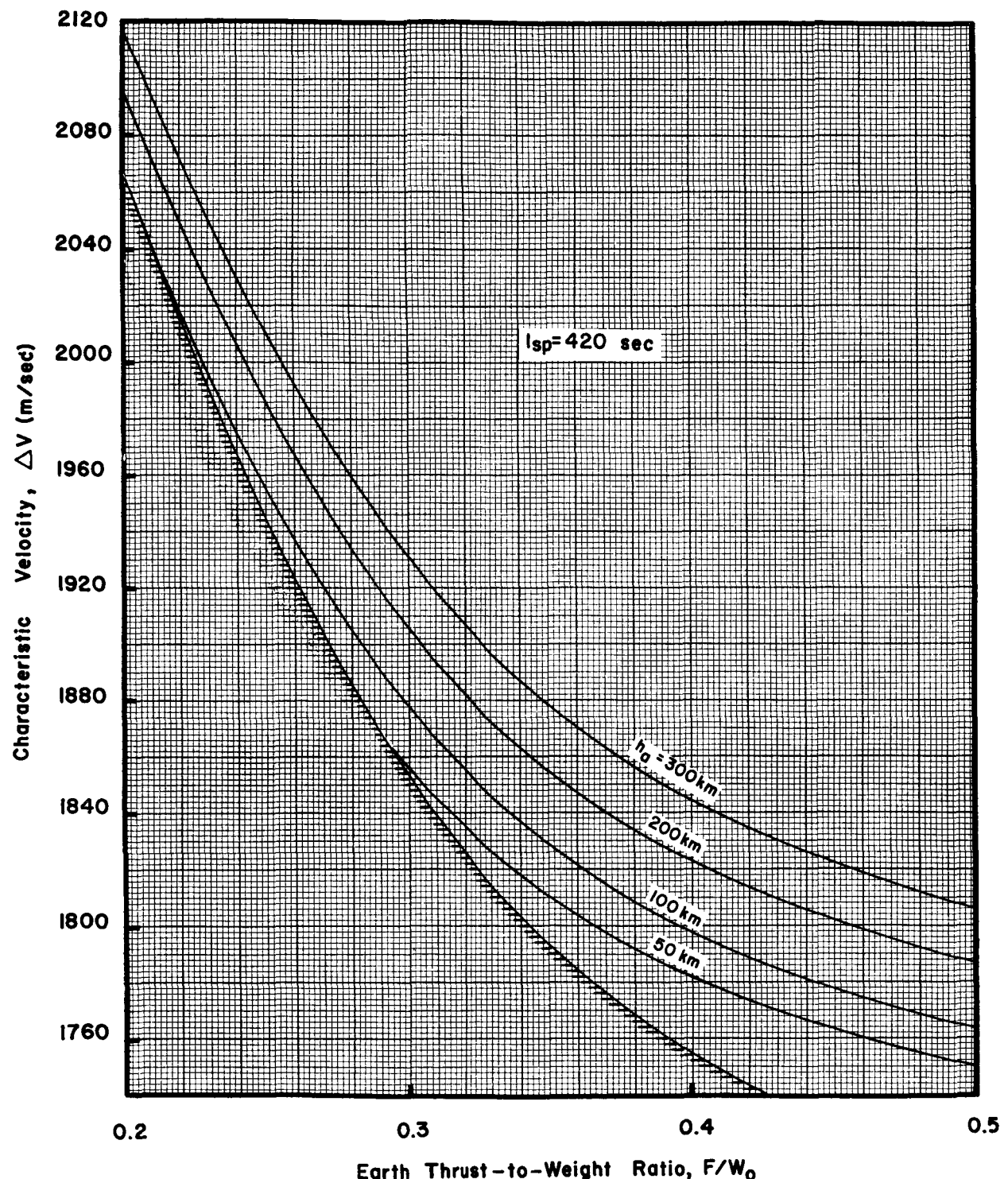


FIGURE 5b. CHARACTERISTIC VELOCITY FOR LUNAR DESCENT - $I_{sp} = 420 \text{ sec.}$

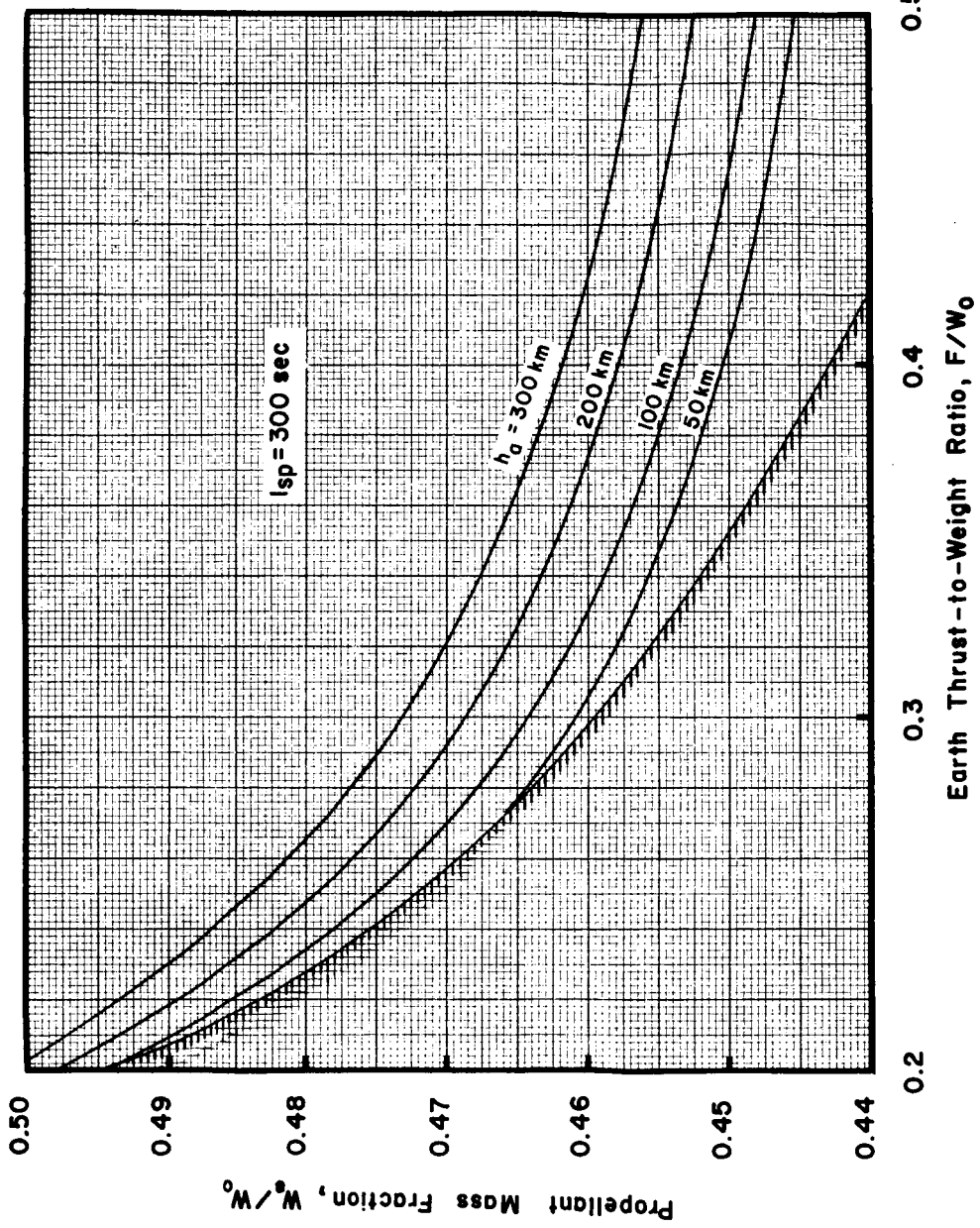


FIGURE 6a. PROPELLANT MASS FRACTION FOR LUNAR DESCENT - $I_{sp} = 300$ sec.

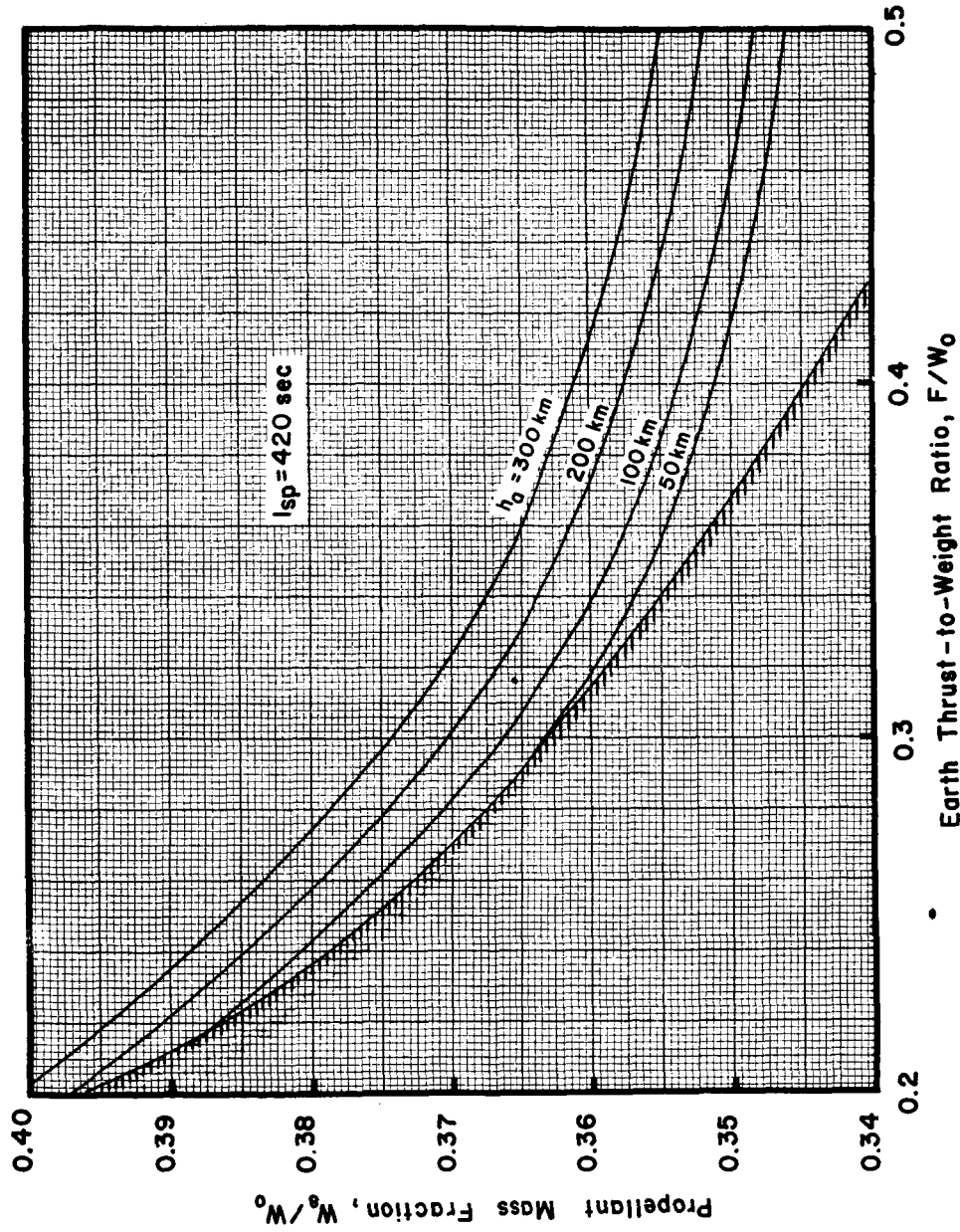


FIGURE 6b. PROPELLANT MASS FRACTION FOR LUNAR DESCENT - $I_{sp} = 420$ sec.

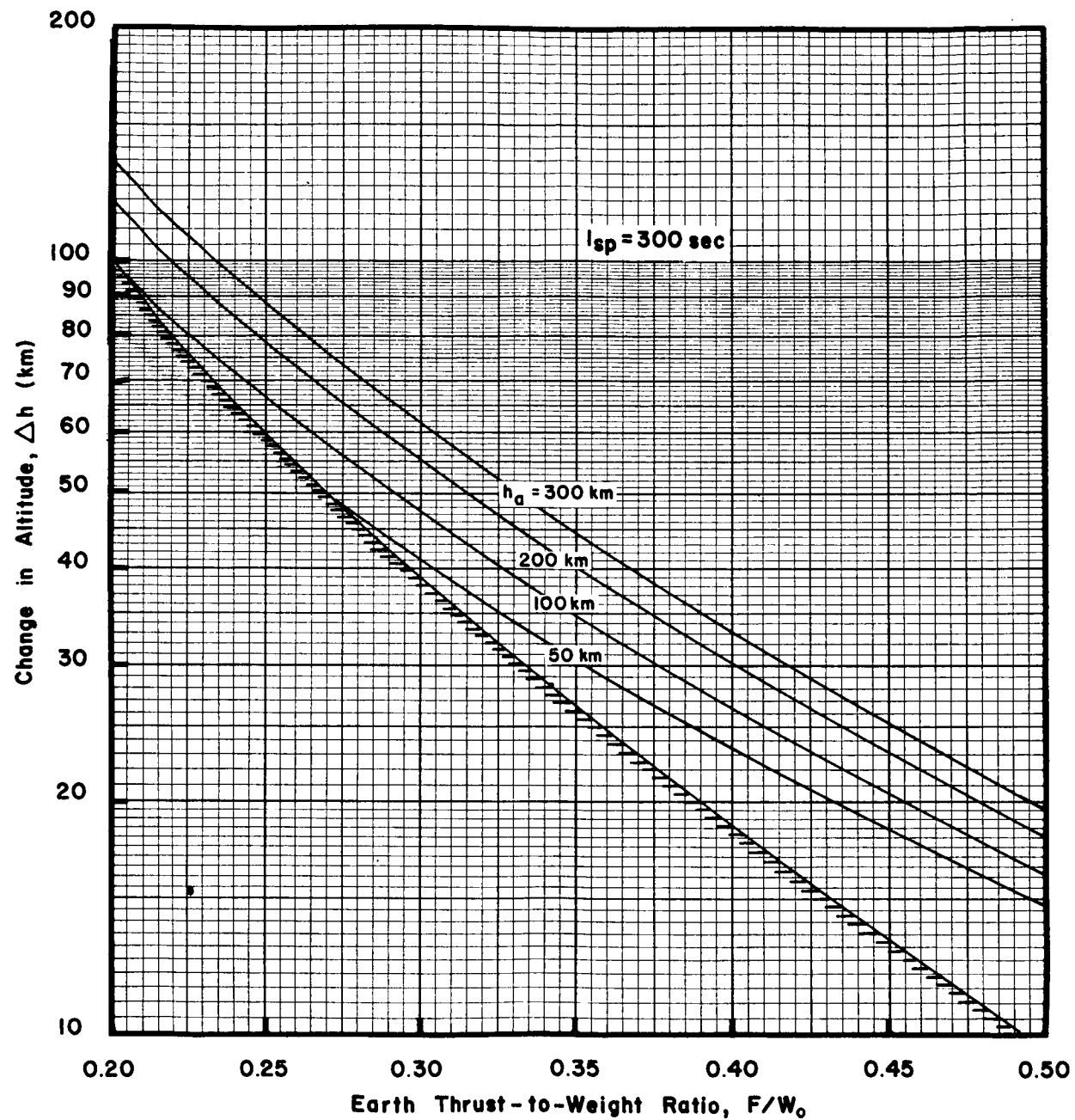


FIGURE 7a. CHANGE IN ALTITUDE FOR LUNAR DESCENT - $I_{sp} = 300$ sec.

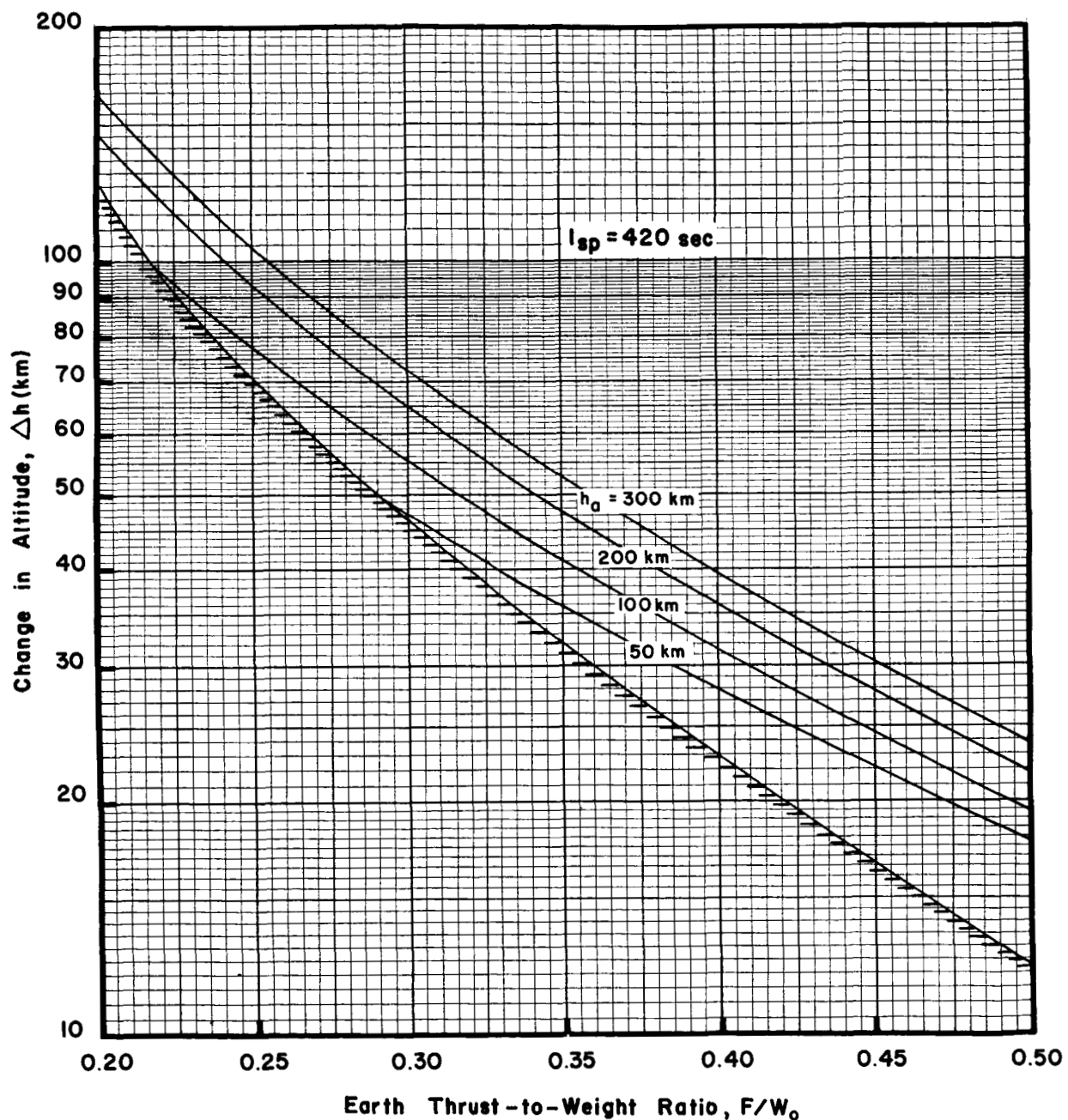


FIGURE 7b. CHANGE IN ALTITUDE FOR LUNAR DESCENT - $I_{sp} = 420 \text{ sec.}$

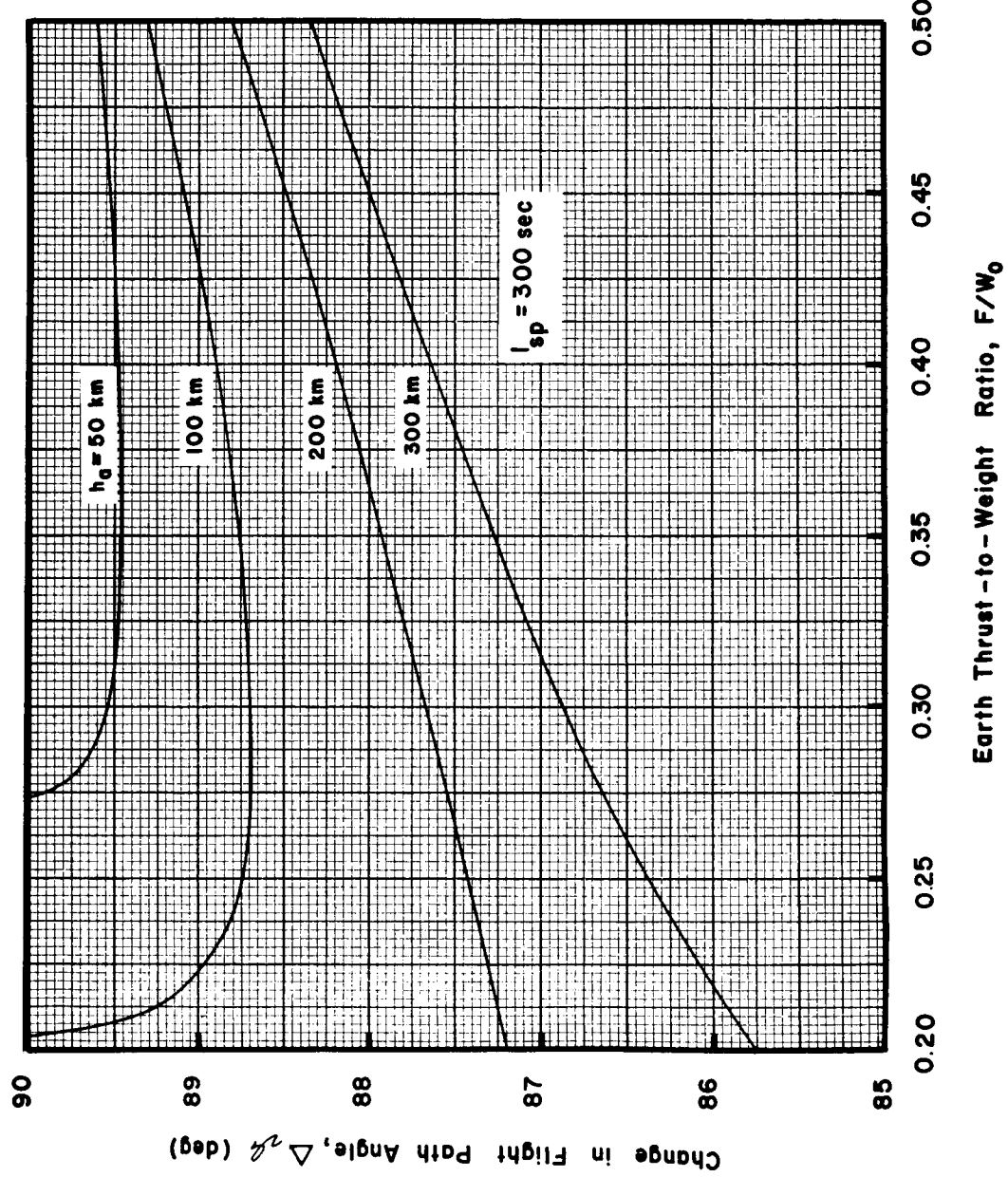


FIGURE 8a. CHANGE IN FLIGHT PATH ANGLE FOR LUNAR DESCENT - $I_{sp} = 300$ sec.

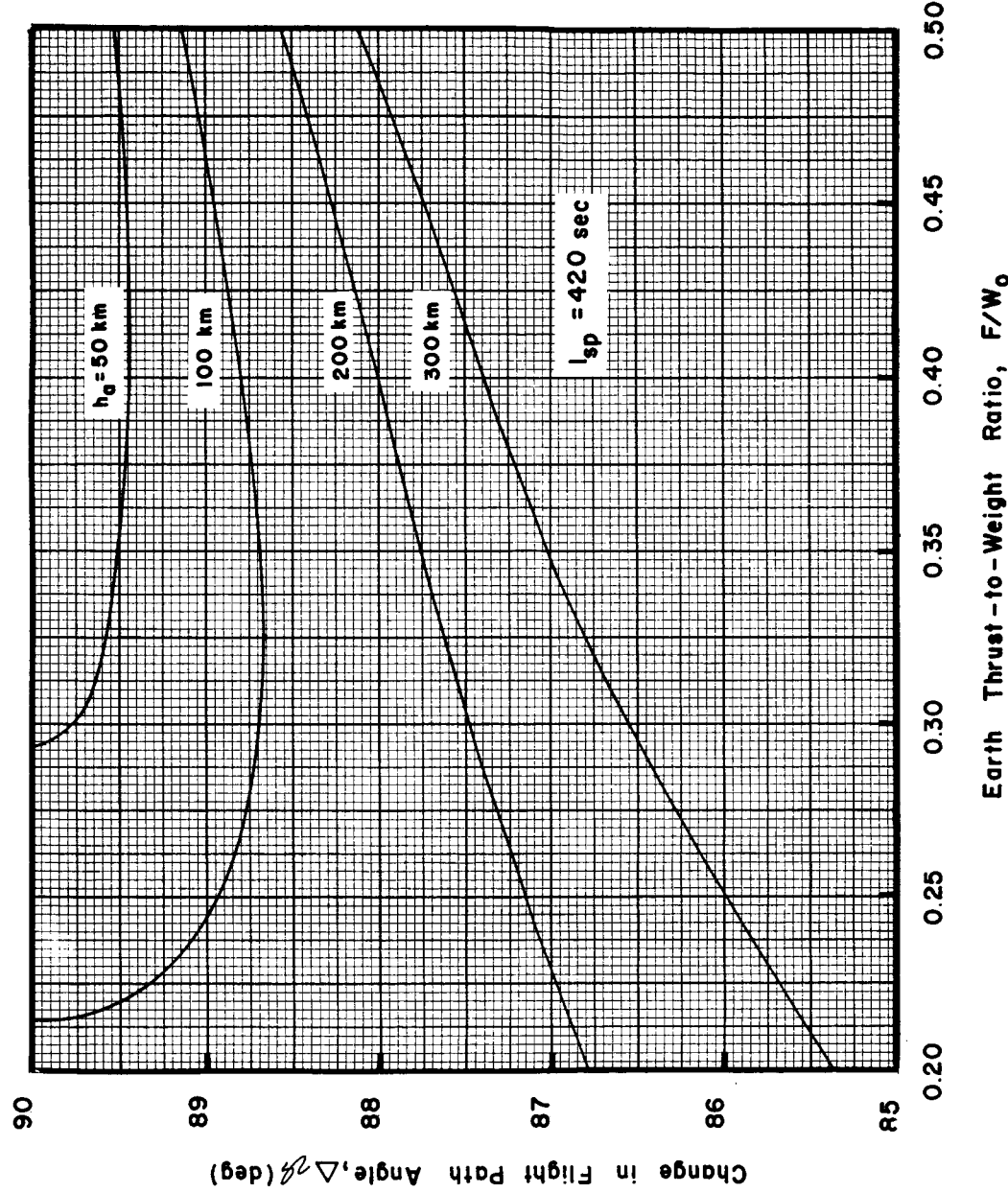


FIGURE 8b. CHANGE IN FLIGHT PATH ANGLE FOR LUNAR DESCENT - $I_{sp} = 420$ sec.

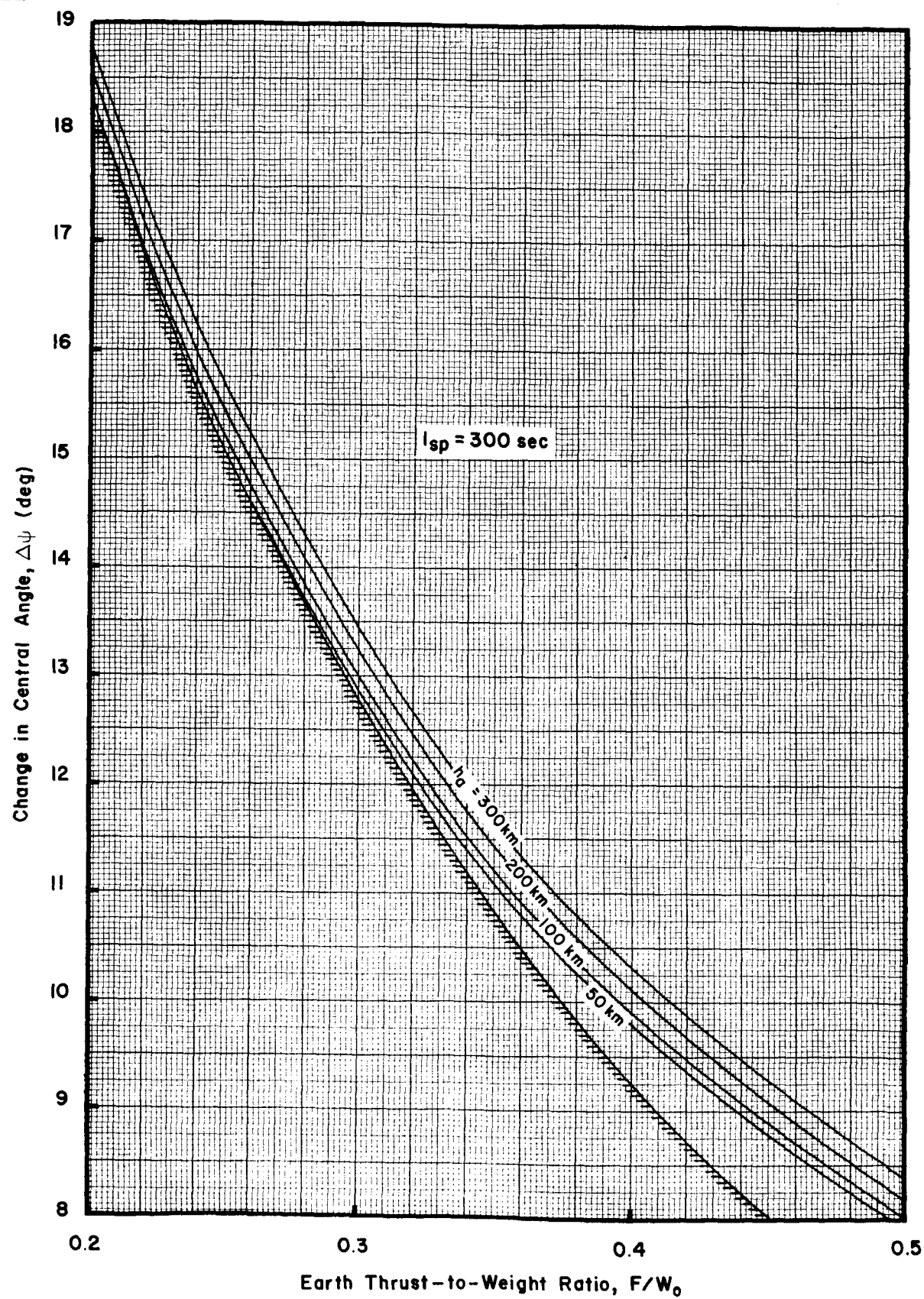


FIGURE 9a. CHANGE IN CENTRAL ANGLE FOR LUNAR DESCENT - $I_{sp} = 300 \text{ sec.}$

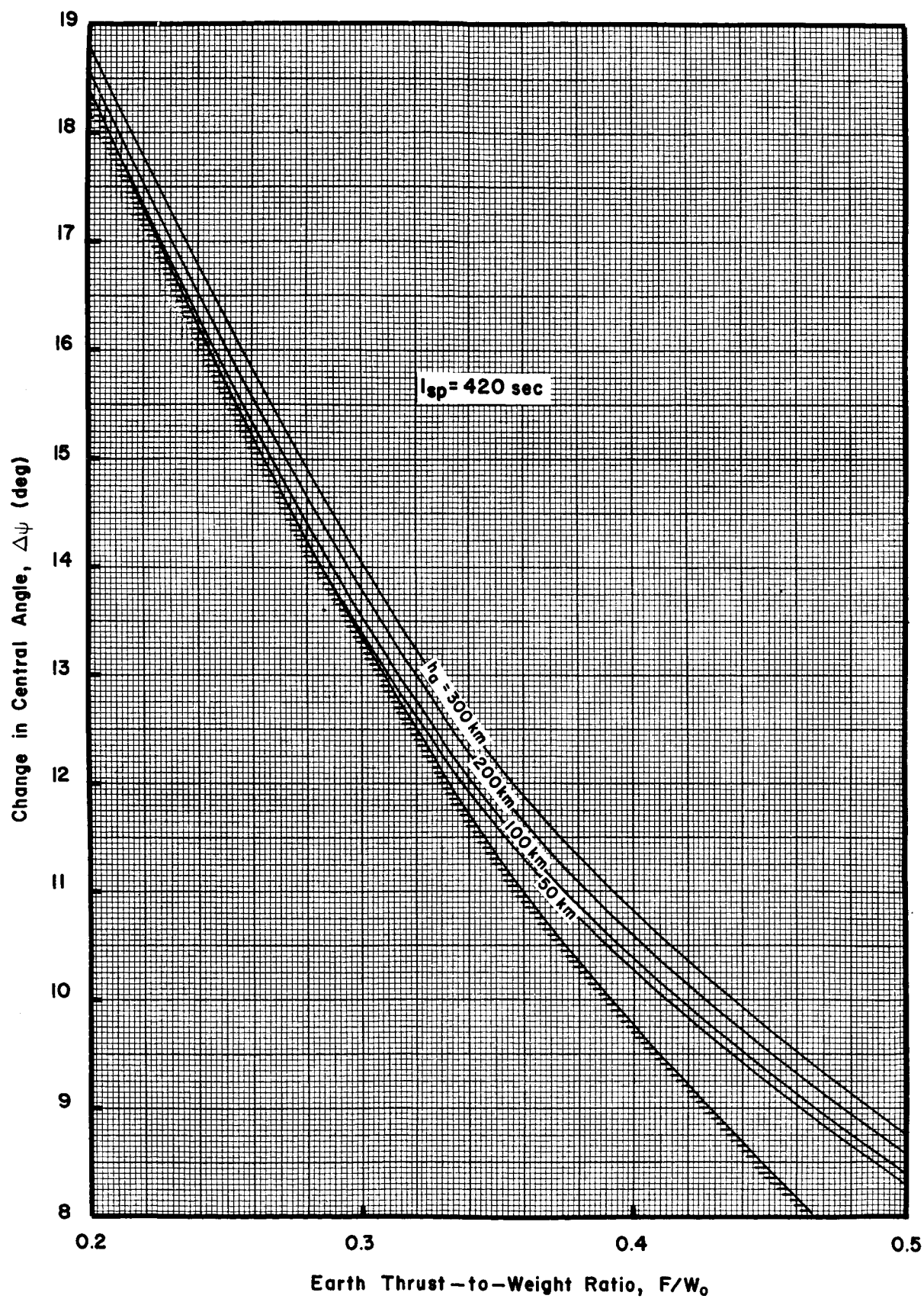


FIGURE 9b. CHANGE IN CENTRAL ANGLE FOR LUNAR DESCENT - $I_{sp} = 420 \text{ sec.}$

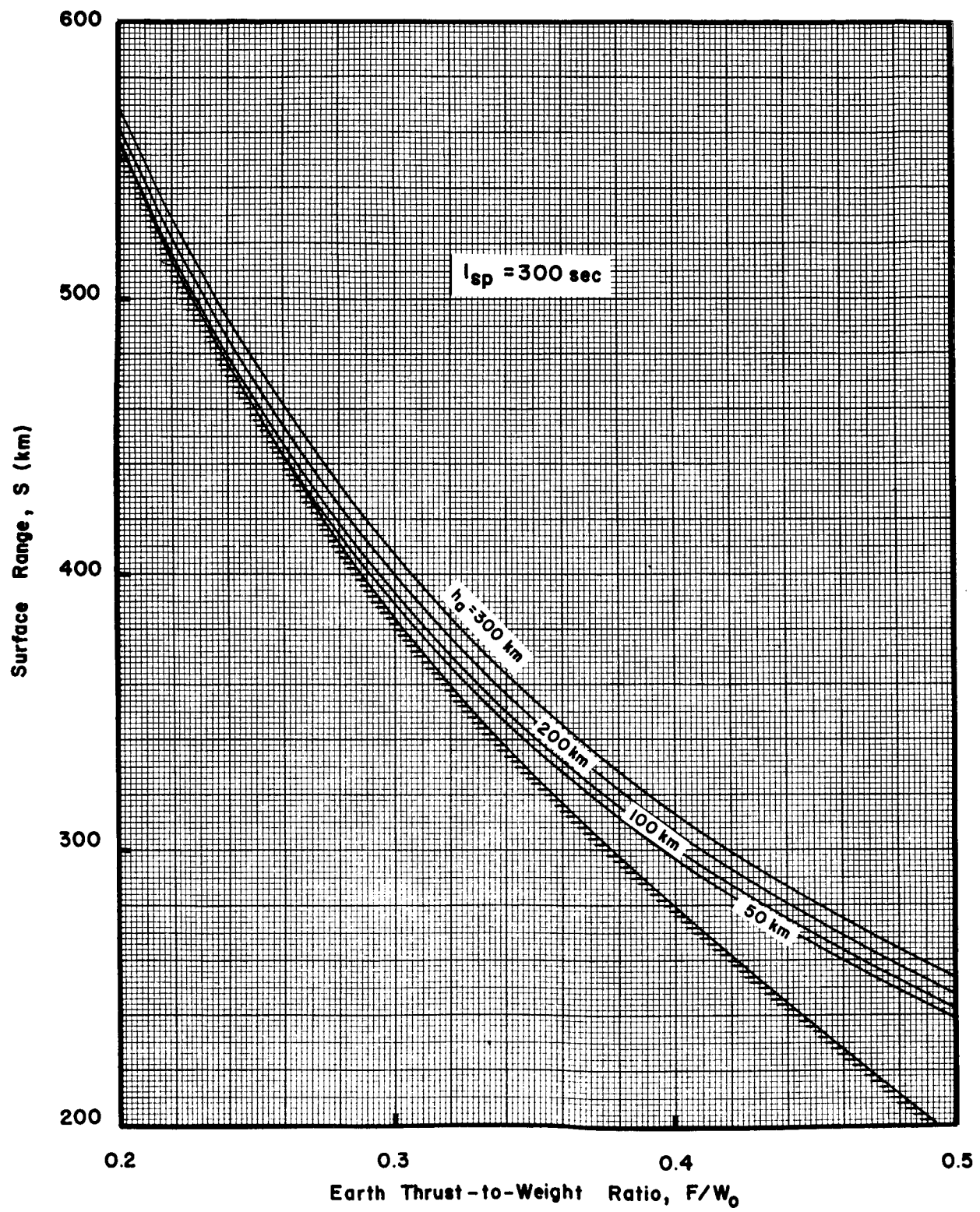


FIGURE 10a. SURFACE RANGE FOR LUNAR DESCENT - $I_{sp} = 300$ sec.

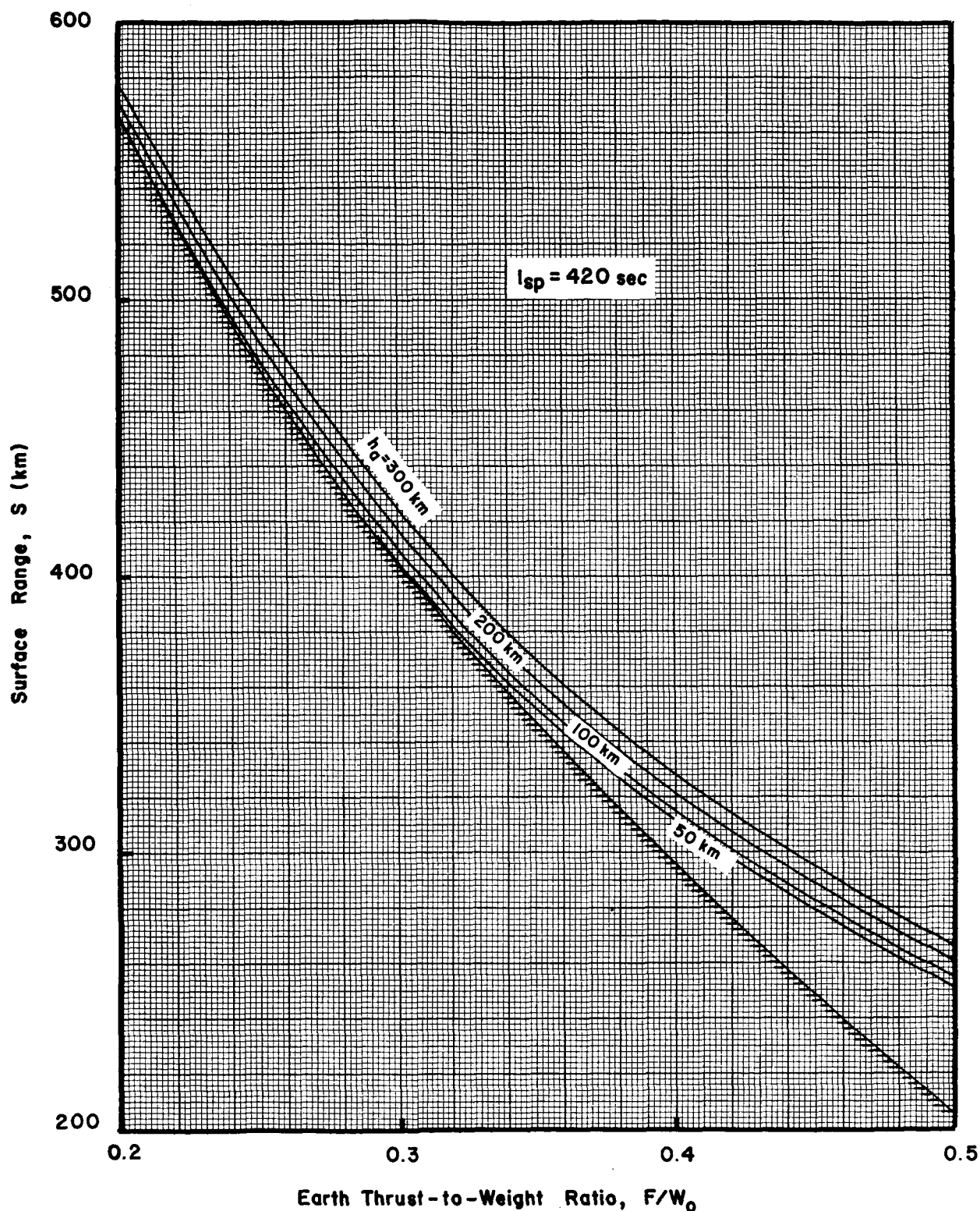


FIGURE 10b. SURFACE RANGE FOR LUNAR DESCENT - $I_{sp} = 420 \text{ sec.}$

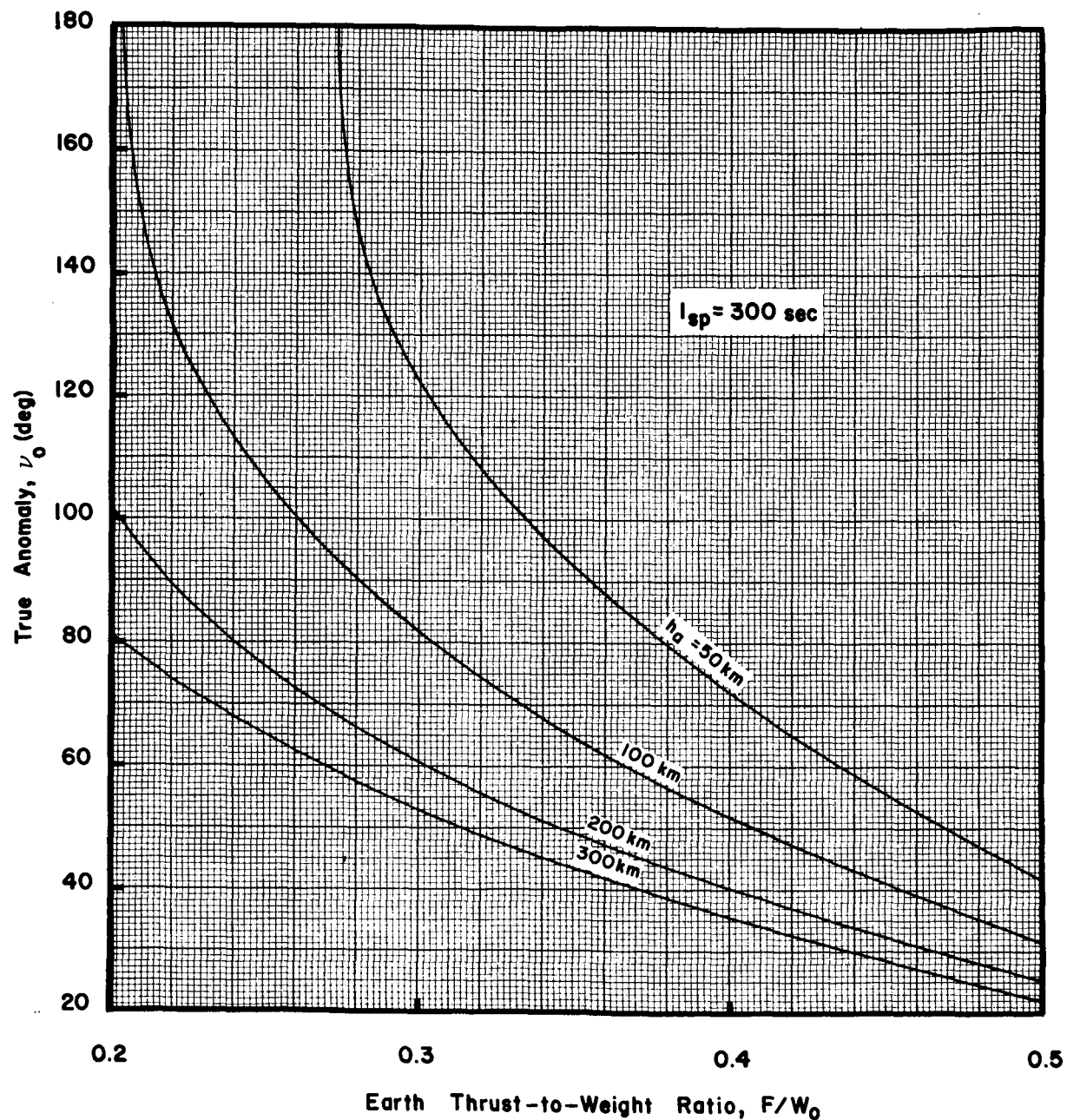


FIGURE 11a. TRUE ANOMALY AT INITIATION OF LUNAR DESCENT - $I_{sp} = 300 \text{ sec.}$

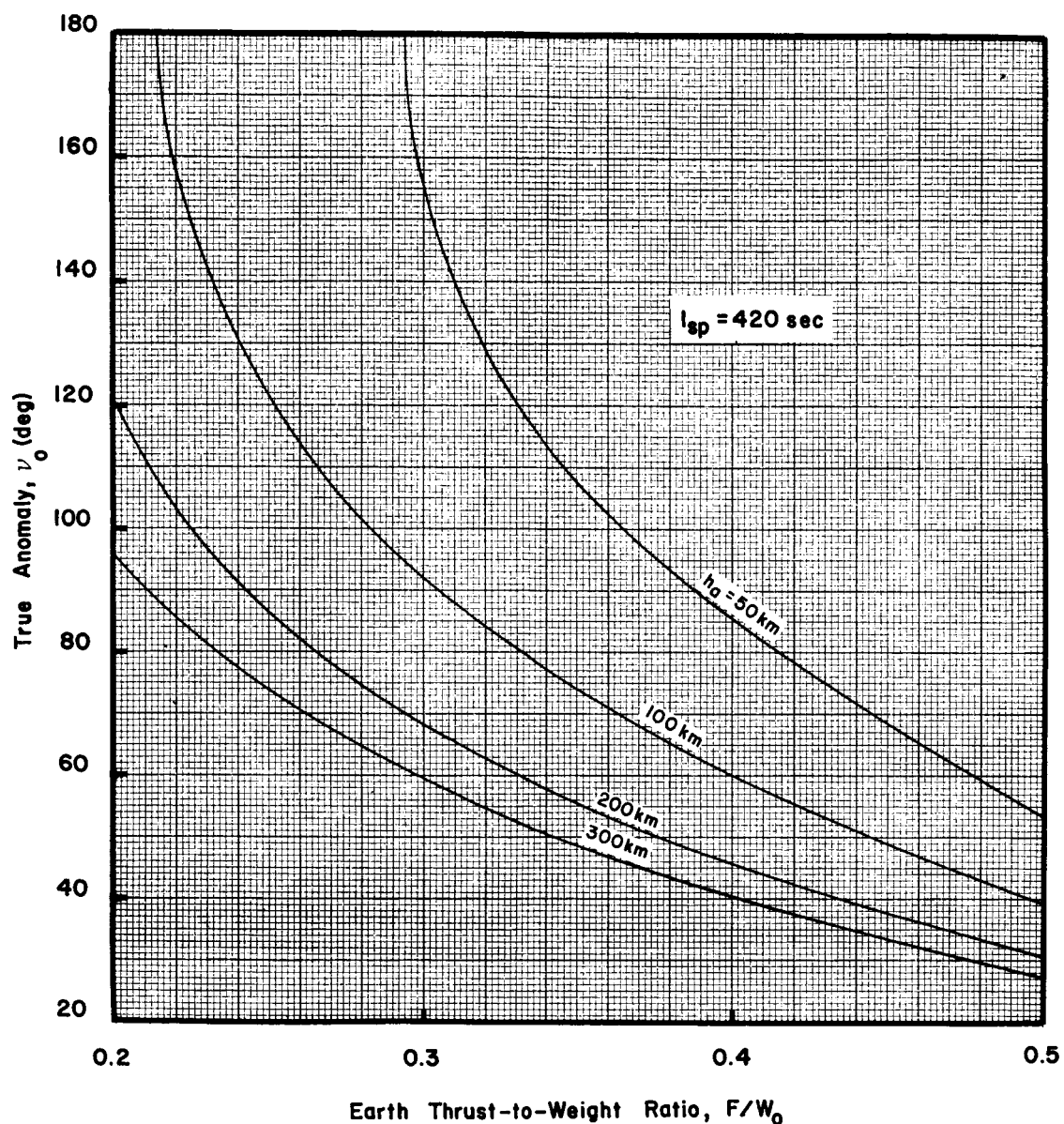


FIGURE 11b. TRUE ANOMALY AT INITIATION OF LUNAR DESCENT - $I_{sp} = 420$ sec.

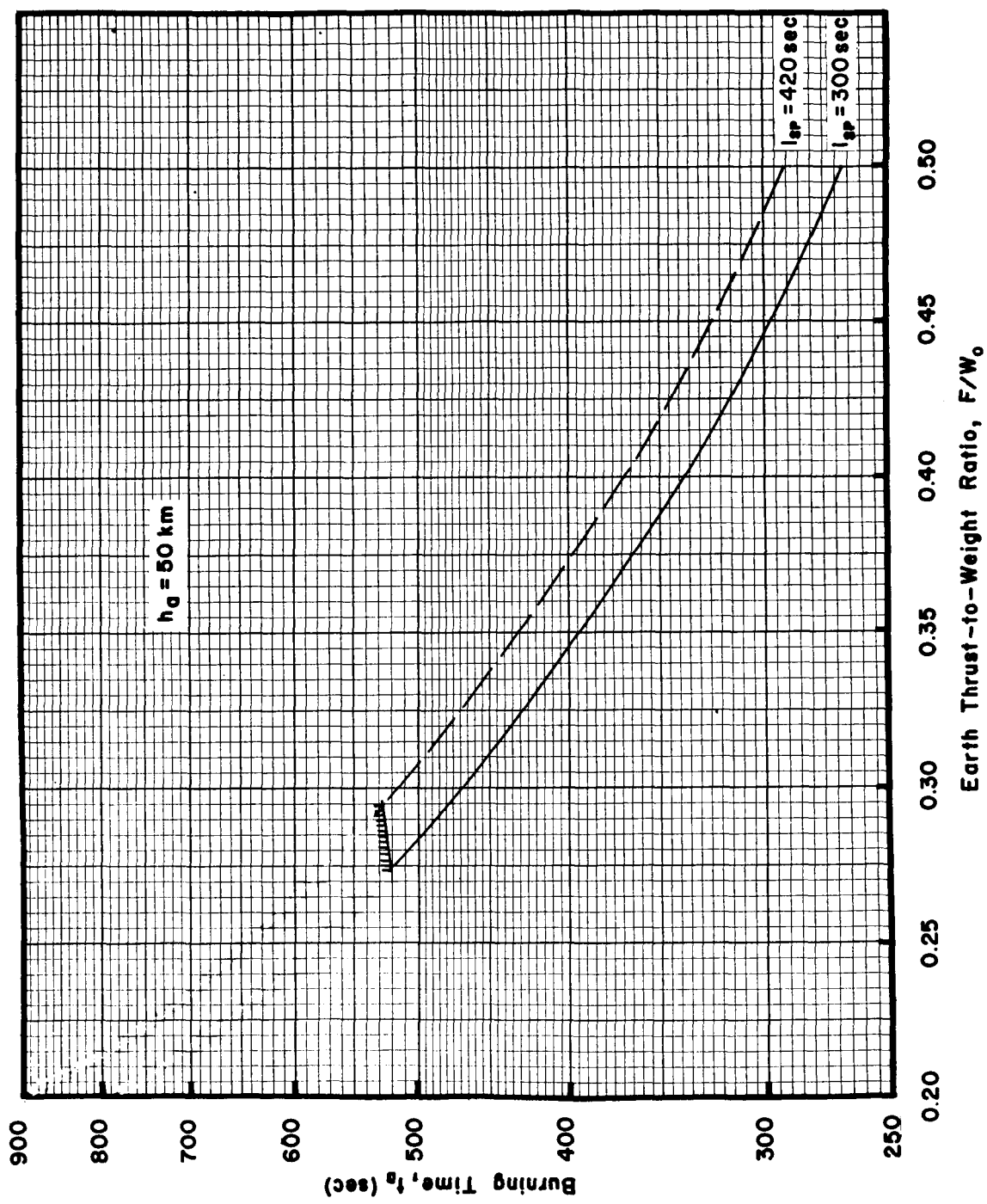


FIGURE 12a. BURNING TIME FOR LUNAR DESCENT - $h_a = 50$ km

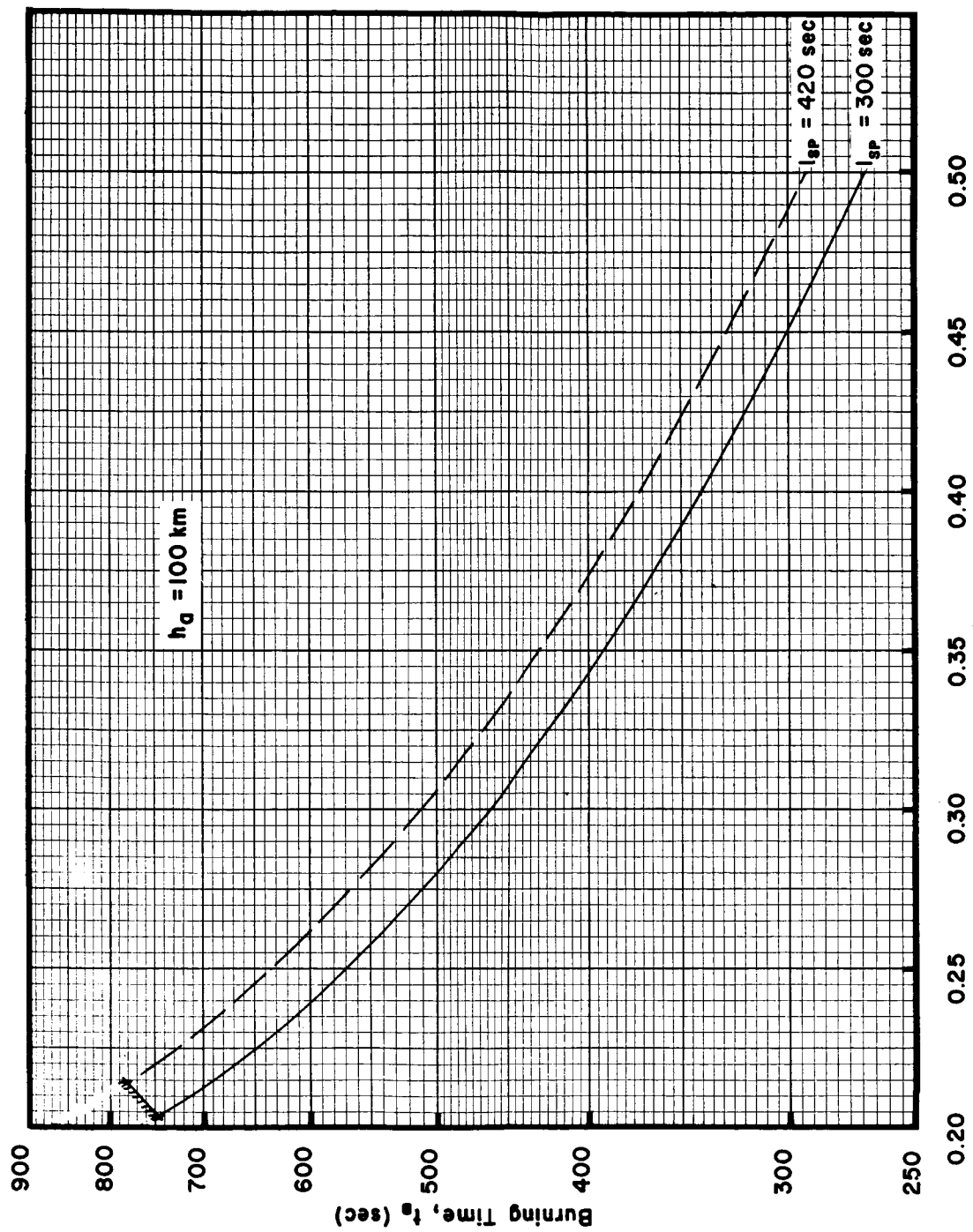


FIGURE 12b. BURNING TIME FOR LUNAR DESCENT - $h_a = 100$ km

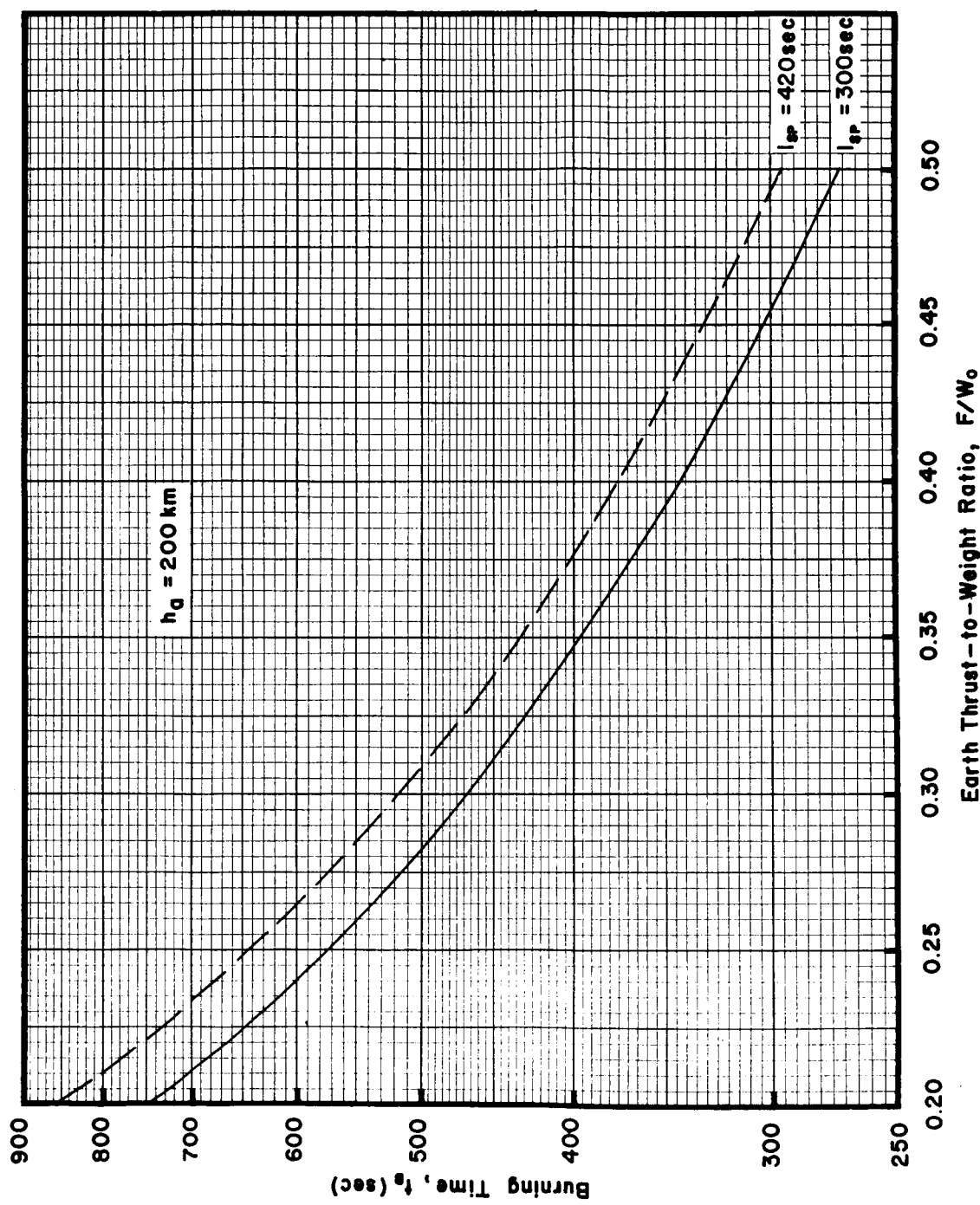


FIGURE 12c. BURNING TIME FOR LUNAR DESCENT - $h_a = 200$ km

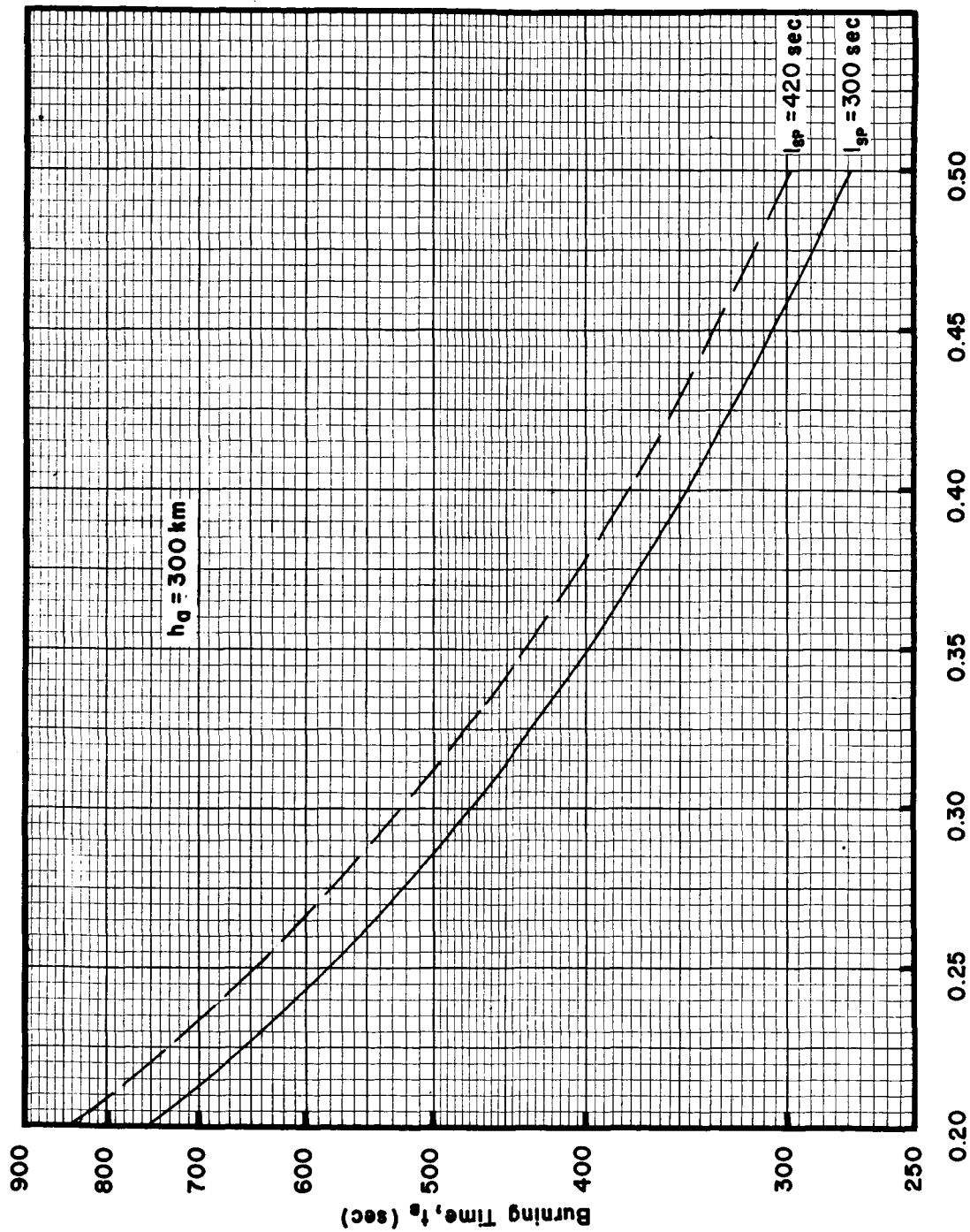


FIGURE 12d. BURNING TIME FOR LUNAR DESCENT - $h_a = 300$ km

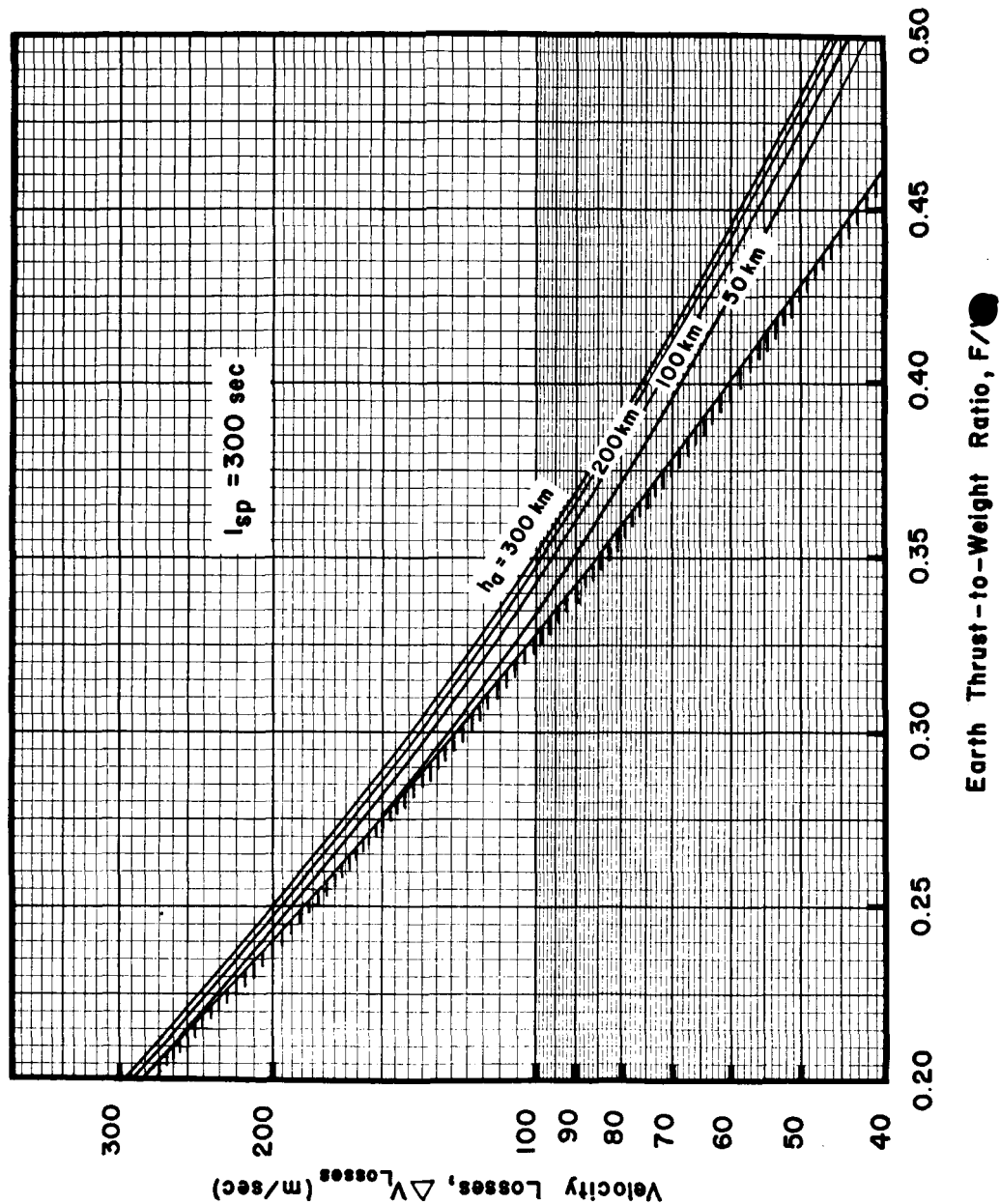


FIGURE 13a. VELOCITY LOSSES FOR LUNAR DESCENT - $I_{\text{sp}} = 300$ sec.

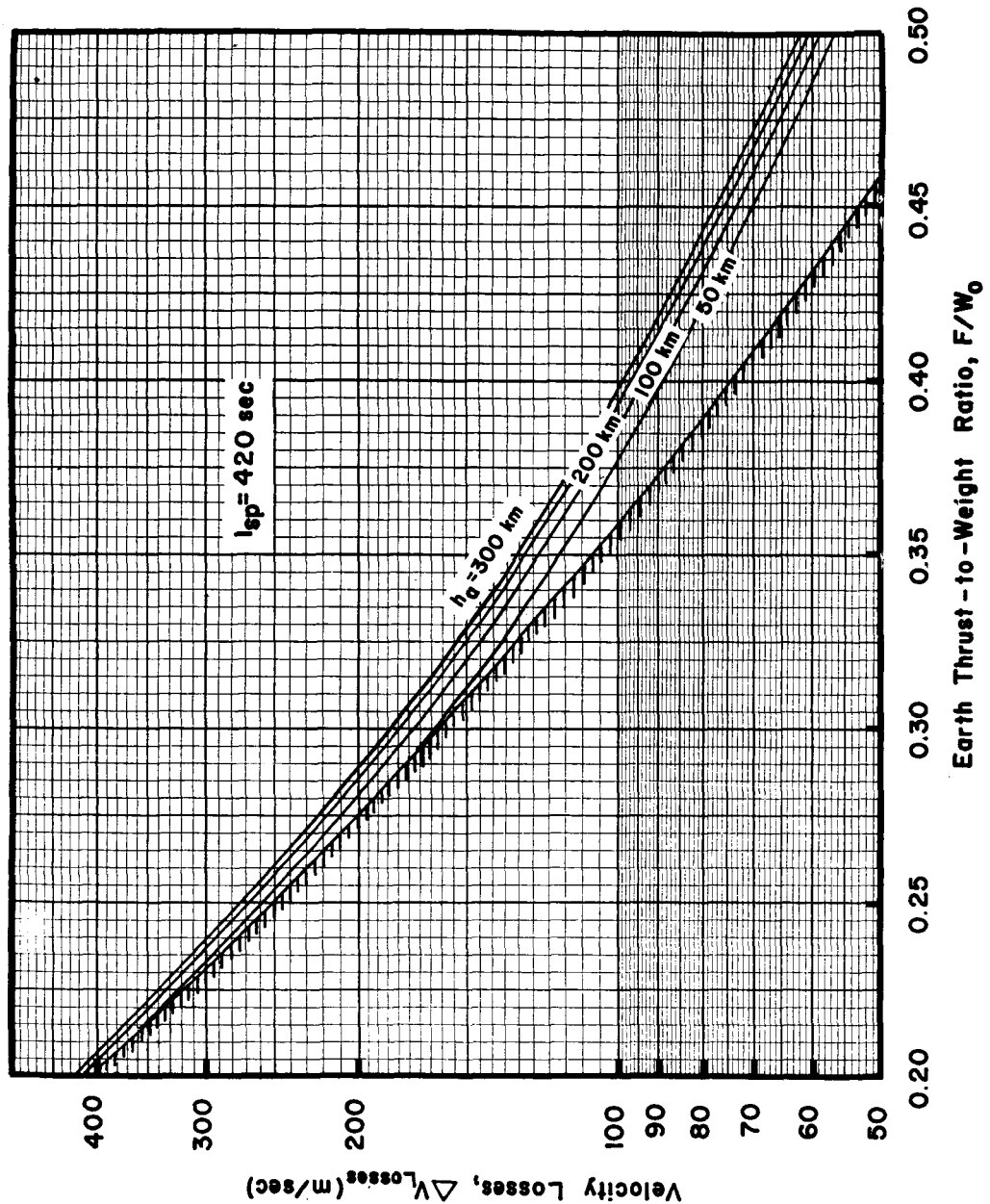


FIGURE 13b. VELOCITY LOSSES FOR LUNAR DESCENT - $I_{\text{sp}} = 420$ sec.

BIBLIOGRAPHY

Akridge, C. M. and Harlin, Sam H., Parametric Performance Analysis of Lunar Missions, Brake to Lunar Orbit. MTP-P&VE-F-63-6, March 5, 1963.

Fellenz, Dietrich W. and Harris, Ronald J., Influence of Weight Parameters on the Propulsion Requirements of Orbit-Launched Vehicles. NASA TN D-1525, May 1963.

Harris, Ronald J. and Austin, R. E., Orbit-Launched Nuclear Vehicle Design and Performance Evaluation Procedure for Escape and Planetary Missions. MTP-P&VE-F-62-11, November 8, 1962.

Jenkins, M. V. and Munford, R. E., Preliminary Survey of Retrograde Velocities Required for Insertion into Low-Altitude Lunar Orbits. NASA TN D-1081, September 1961.

Mason, Maxwell and Brainin, S. M., Descent Trajectory Optimization for Soft Lunar Landings. IAS 30th Annual Meeting. Paper No. 62-11, January 22-24, 1962.

Queijo, M. J. and Miller, G. K. Jr., Analysis of Two Thrusting Techniques for Soft Lunar Landings Starting from a 50-mile Altitude Circular Orbit. NASA TN D-1230, March 1962.

Stafford, Walter H., Working Graphs for Artificial Lunar Satellites. IN-P&VE-F-62-6, July 3, 1962.

Steiner, P., Lunar Powered Flight. STL Report No. 8976-0004-RU-000, August 10, 1961.

Weber, R. J., Pauson, W. M. and Burley, R. R., Lunar Trajectories. NASA TN D-866, August 1961.

Weber, R. J. and Pauson, W. M., Some Thrust and Trajectory Considerations for Lunar Landings. NASA TN D-134, November 1959.

APPROVAL

MTP-P&VE-F-63-8

PARAMETRIC PERFORMANCE ANALYSIS OF LUNAR MISSIONS

PART II

LUNAR DESCENT

By Charles M. Akridge and Sam H. Harlin

The information in this report has been reviewed for security classification. Review of any information concerning Department of Defense or Atomic Energy Commission programs has been made by the MSFC Security Classification Officer. This report, in its entirety, has been determined to be unclassified.

James W. Russell
J. W. RUSSELL
Chief, Orbital and Re-entry Flight Unit

A. W. Galvezano
A. W. GALVEZANO
Acting Chief, Flight Operations Section

Rich J. Price.
ERICH E. GOERNER
Chief, Advanced Flight Systems Branch

W. A. Mrazek
W. A. MRAZEK
Director, Propulsion and Vehicle Engineering Division

DISTRIBUTION

M - DIR	M - AERO - P
Dr. von Braun	Dr. Hoelker
	Mr. Dearman
M - DEP - R&D	M - ASTR - DIR
Dr. Rees	Dr. Haeussermann
M - CP - DIR	M - ASTR - A
Mr. Maus	Mr. Digesu
M - AERO - DIR	M - ASTR - M
Dr. Geissler	Mr. Boehm
M - AERO - S	Mr. Pfaff
Mr. de Fries	
M - AERO - TS	M - COMP - DIR
Mr. Baussus	Dr. Hoelzer
Dr. Heybey	Mr. Bradshaw
Dr. Sperling	
M - AERO - PS	M - FPO
Mr. Braunlich	Mr. Koelle
Mr. Schmidt	Mr. Williams
	Dr. Ruppe
M - AERO - A	M - MS - H
Mr. Dahm	Mr. Akens
Mr. Struck	
Mr. Linsley	M - MS - IP
	Mr. Remer
M - AERO - D	M - P&VE - DIR
Mr. Horn	Dr. Mrazek
Mr. Thomae	Mr. Weidner
Mr. Callaway	Mr. Hellebrand
Mr. Scott	
M - AERO - F	M - P&VE - V
Dr. Speer	Mr. Palaoro
Mr. Kurtz	
	M - P&VE - M
	Dr. Lucas

DISTRIBUTION (Concluded)

M-P&VE-F	M-P&VE-SA
Mr. Goerner	Mr. Blumrich
Mr. Barker	Mr. Engler
Mr. Swanson	
Dr. Krause	M-P&VE-E
Mr. Burns	Mr. Schulze
M-P&VE-FN	M-P&VE-ADMP
Mr. Jordan	
Mr. Harris	M-RP-DIR
Mr. Saxton	Dr. Stuhlinger
Mr. Manning	Mr. Heller
M-P&VE-FF	M-RP
Mr. Galzerano	Mr. Snoddy
Mr. Fellenz	Mr. Prescott
Mr. Kromis (5)	Mr. Naumann
Mr. Russell	Mr. Fields
Mr. Akridge (25)	
Mr. Harlin	M-SAT-DIR
Mr. Thompson	Dr. Lange
Mr. Stafford	
Mr. Perry	M-HME-P
	Mr. Knox
M-P&VE-FS	M-MS-IPL
Mr. Neighbors	Miss. Robertson (8)
Mr. Johns	
Mr. Orillion	M-PAT
Mr. Schwartz	Scientific and Technical Information
Mr. Laue	Facility
M-P&VE-P	Attn: NASA Representatives (2)
Mr. Paul	(S-AK/RKT)
Mr. Head	P. O. Box 5700
M-P&VE-S	Bethesda, Maryland
Mr. Kroll	
Dr. Glaser	